The Effect of Several Infrared Transparent Broadening Gases on the Absorption of Infrared Radiation in the 15μm Band of Carbon Dioxide

CASE FILE COPY

HENRY GEORGE REICHLE, JR.

May 1969

High Altitude Engineering Laboratory

THE UNIVERSITY OF MICHIGAN
COLLEGE OF ENGINEERING
High Altitude Engineering Laboratory
Departments of
Aerospace Engineering
Meteorology and Oceanography

Technical Report

THE EFFECT OF SEVERAL INFRARED TRANSPARENT BROADENING GASES ON THE ABSORPTION OF INFRARED RADIATION IN THE 15μm BAND OF CARBON DIOXIDE

ORA Project 05863

May 1969

THE EFFECT OF SEVERAL INFRARED TRANSPARENT BROADENING GASES ON THE

ABSORPTION OF INFRARED RADIATION IN THE 15 μm BAND OF CARBON DIOXIDE

by
Henry George Reichle, Jr.

A dissertation submitted in partial fulfillment
of the requirements for the degree of
Doctor of Philosophy in
The University of Michigan
1969

Doctoral Committee:

      Associate Professor Frederick L. Bartman, Chairman
      Associate Professor Edward A. Boettner
      Professor Leslie M. Jones
      Assistant Professor William R. Kuhn
      Assistant Professor Charles Young, The University of New Brunswick

ACKNOWLEDGMENTS

As is the case in most investigations of this type, the work reported here is the result of the efforts of many people. The author would like to thank all of those who contributed. The advice and help of Professor Frederick Bartman, Chairman of the Doctoral Committee and Professor Charles Young of the University of New Brunswick, whose advice during the early part of the investigation and during the data analysis was most helpful, are particularly appreciated. The author is also grateful to Professors Edward Boettner, Leslie Jones, and William Kuhn for serving as members of the Committee and for their help and suggestions during the course of the work.

The help of the staff of the High Altitude Engineering Laboratory is appreciated. Among them the author would most like to thank Mr. Charles Hubler, whose assistance in all phases of this investigation was of great value.

The financial support received from the Goddard Space Flight Center of the National Aeronautics and Space Administration under contract NASr-54(03) and the loan of the spectrophotometer by the Langley Research Center of the National Aeronautics and Space Administration is acknowledged.

Finally the author would like to thank his wife for her patience, encouragement, and financial support and the other members of his family (including Mrs. Donald Reichle, who typed this paper) for their encouragement and help.

TABLE OF CONTENTS

TABLE OF CONTENTS (Concluded)

LIST OF TABLES

LIST OF FIGURES

LIST OF FIGURES (Concluded)

LIST OF SYMBOLS

a	a constant
A	equivalent width
A_ν	wavenumber dependent absorptivity
B	broadening coefficient
B'	mean value of the wavenumber dependent broadening coefficient
B_{avg}	average value of the broadening coefficient
B_i	broadening coefficient for gas i
B_A	broadening coefficient for argon
B_{He}	broadening coefficient for helium
B_{N_2}	broadening coefficient for nitrogen
B_{O_2}	broadening coefficient for oxygen
c	speed of light
C	absorber concentration
C_{aa}	constant involving collision diameter and molecular weight of an absorber
C_{ab}	constant involving collision diameter and molecular weights of an absorber and a broadener
D_{aa}	optical collision diameter for collisions of the absorber with itself
D_{ab}	optical collision diameter for collisions of the absorber with a broadening gas
D_{aN_2}	optical collision diameter for collisions of the absorber with nitrogen
$D_{CO_2CO_2}$	optical collision diameter for collisions between carbon dioxide molecules

$D_{CO_2 b}$	optical collision diameter for collisions between carbon dioxide molecules and a broadening gas
E	extinction coefficient
E	energy
f	frequency
f_o	frequency of the line center
F	broadening factor
F'	broadening factor calculated from the mean value of the wavelength dependent broadening coefficients
F_i	broadening factor for gas i
F_A	broadening factor for argon
F_{He}	broadening factor for helium
F_{N_2}	broadening factor for nitrogen
F_{O_2}	broadening factor for oxygen
h	Planck's constant
I	intensity of the transmitted radiation
I_o	intensity of the incident radiation
k	Boltzmann's constant
k_f	absorption coefficient at frequency f
k_o	absorption coefficient at the line center
k_ν	absorption coefficient at wavenumber ν
l	path length
l	cell length
m	mass

M_a	molecular weight of the absorbing molecule
M_b	molecular weight of the broadening molecule
N_a	number density of the absorbing gas
N_b	number density of the broadening gas
P_a	partial pressure of the absorbing gas
P_b	partial pressure of the broadening gas
P_e	effective pressure
P_i	partial pressure of gas i
P_x	calibration pressure
P_A	argon partial pressure
P_{CO_2}	carbon dioxide partial pressure
P_{He}	helium partial pressure
P_{N_2}	nitrogen partial pressure
P_{O_2}	oxygen partial pressure
P_e^L	effective pressure in the long cell
P_e^S	effective pressure in the short cell
$P_{CO_2}^L$	carbon dioxide partial pressure in the long cell
$P_{CO_2}^S$	carbon dioxide partial pressure in the short cell
S	a constant generally called the line strength
t	time
T	temperature

T_{cell}	transmissivity of the sample cell relative to the transmissivity of the reference cell
T_{ind}	transmissivity as indicated by the spectrophoto-meter
$T_{reference\ cell}$	transmissivity of the cell in the reference beam
$T_{sample\ cell}$	transmissivity of the cell in the sample beam
T_{ν}	wavenumber dependent transmissivity
V	particle velocity
w	optical mass
Z_{off}	zero offset
α	line half width at half maximum
α_D	Doppler halfwidth
α_L	Lorentz halfwidth
α_N	natural halfwidth
λ	wavelength
μ	Dipole moment
ν	wavenumber
ν_{min}	minimum wavenumber
ν_{max}	maximum wavenumber
τ	mean time between molecular collisions

ABSTRACT

The objective of this investigation is to determine the effects

of argon, helium, nitrogen and oxygen on the absorption of radiation

by carbon dioxide in the 15μm (667 cm^{-1}) region. The investigation

is carried out at medium resolution (approximately 3 to 5 cm^{-1}) and

at gas pressures that are less than one atmosphere. After a review

of previous experimental and theoretical work pertinent to the

investigation the expressions defining the broadening coefficient

and the broadening factor are given. The experimental apparatus

used to measure the effects of the various broadening gases is

described and the experimental procedure is discussed. The results

of the investigation are presented in the form of a band averaged

broadening coefficient for nitrogen, band averaged broadening

factors for argon, helium and oxygen, and wavelength dependent

broadening coefficients for argon, helium, nitrogen and oxygen.

It is found that the band averaged broadening coefficient for

nitrogen and the band averaged broadening factors for argon and

oxygen are in good agreement with previous experimental results

in other carbon dioxide absorption bands. The band averaged value

of the broadening factor for helium, however, is found to be sig-

nificantly higher than values previously obtained in the 2350cm^{-1}

band.

The wavelength dependent broadening coefficients are found

to be more complex in structure than previous determinations have

indicated. It is noted that the broadening coefficients for argon, nitrogen and oxygen are qualitatively similar to each other but are quite different from the broadening coefficient for helium. It is shown that the fine structure of the wavelength dependent broadening coefficient is correlated with the presence of several absorption bands having strong Q branches in the 15μm region. Comparisons of the mean values of the wavelength dependent broadening coefficients are used to substantiate the previously determined values of the band averaged broadening factors.

The wavelength dependent broadening coefficient for nitrogen is compared to previously calculated theoretical predictions of this quantity. It is shown that, although Anderson's theory successfully predicts the mean value and general features of the wavelength dependent broadening coefficient, it fails to predict the sharp peaks in the broadening coefficient that are observed in the vicinity of the frequencies of the main Q branches. On the basis of a qualitative argument it is shown that the peaking of the broadening coefficient in the vicinity of Q branches and the unusual behavior of the broadening coefficient for helium could be explained by deviations of the line shape from the theoretical line profile similar to those that have been observed in other carbon dioxide absorption bands or by a variation of the line half width with rotational quantum number.

CHAPTER 1

INTRODUCTION

The advent of the sounding rocket, the earth orbiting satellite and the interplanetary spacecraft has placed in the hands of meteorologists and atmospheric scientists powerful new tools for measuring the characteristics of planetary atmospheres. The effective use of these devices often involves inferring the desired information from remotely sensed data. At the present time, one very widely used technique involves scanning a planetary atmosphere using radiometers, spectrometers or interferometers operating in the infrared region ($1-50\mu m$). This spectral region is of great interest because the black body emission of the planetary surface peaks at these wavelengths, and because some important gases present in planetary atmospheres e.g., water vapor, carbon dioxide and ozone, have strong absorption bands in this spectral region. Furthermore, the distribution of these gases, with their strong absorption bands, influences the temperature structure of the atmosphere. Before the properties of the planetary atmosphere can be properly inferred from the remotely sensed data or the atmospheric structure can be properly understood, it is necessary to have a complete understanding of the radiative transfer problem for the atmosphere. This involves an accurate knowledge of the transmission properties of the infrared optically active gases.

In the past the transmission properties of the atmospheric gases have generally been obtained using idealized mathematical models, called band models. A band model, for example, assumes some distri-

bution of absorption lines which enables the transmission to be readily obtained analytically and is primarily used to facilitate hand solution of the radiative transfer problem. The models have become inadequate because of their basic limitations and fundamental inaccuracies, particularly, as the problem of translating measurements taken at satellite altitudes into knowledge of the atmospheric structure has become better known. The high speed digital computer with large information storage capability has, however, made it possible to calculate the transmission properties of a gas directly from knowledge of the positions, shapes, strengths and widths of the absorption lines comprising an absorption band. Unfortunately, much of the very accurate information required for calculations of this type is not available at the present time. Most of the existing theoretical and experimental work has been done for highly polar molecules such as hydrogen chloride. Generally, the data have been obtained for samples of pure gas or for samples using nitrogen as a broadening gas, the data for broadening by other transparent gases being very limited. Since the gases that are active in the infrared region are trace constituents in the atmosphere of the earth, it is important that the effects of the other atmospheric gases on the absorption properties of the optically active gas be known.

This paper discusses the results of a medium resolution spectroscopic investigation of the effects of several broadening gases on the absorption properties of carbon dioxide in the 15 μm band. The broadening gases used (argon, helium, nitrogen and oxygen) were selected because of their possible importance in the atmosphere of the earth or other planets (argon, nitrogen, and oxygen) or because

of some unusual property (the low mass of helium).

The introduction will be concluded with a review of the litera-
ture concerning previous experimental work on foreign gas broadening
for carbon dioxide. Chapter 2 is devoted to a summary of the theory
of line broadening and the development of a set of semi-empirical
relations that will define experimentally measurable parameters re-
lated to the widths of the absorption lines. The experimental appara-
tus is described in detail in Chapter 3. In Chapter 4 spectra for
nitrogen broadened carbon dioxide samples are presented. These are
compared with spectra obtained by other experimenters under similar
test conditions and with absorption spectra obtained by the direct
computational technique described by Drayson and Young (1966) and
Drayson et al., (1968). Chapters 5 and 6 are devoted to a study of
the band averaged broadening abilities of the gases. Chapter 7 dis-
cusses the wavelength dependence of the broadening ability of the
various gases. Comparisions with the predictions of Anderson's Theory
(Anderson, 1949) for nitrogen as the broadening gas obtained by
Yamamoto et al., (1968) are presented and possible reasons for the
differences between theory and experiment are discussed. The wave-
length dependence of the broadening abilities for the various gases
is compared and possible mechanisms to explain the differences are
offered. The report concludes with Chapter 8 which summarizes the
principal findings of the work and suggests possible areas for future
research efforts.

Although absorption line broadening as a result of the Doppler
effect had been studied earlier, the effects of other perturbing mole-
cules was begun by Michelson (1895). It was his conclusion that the

nature of the perturbing gas would be of secondary importance. The work on foreign gas broadening was continued primarily in Europe until approximately 1940. It was during this interval that it became possible to resolve the structure of the bands and to examine the transmission properties of the gas for more or less monochromatic radiation. A review of the work in the field performed prior to 1944 is given by Nielsen et al., (1944). Coggeshall and Saier (1947) reported the effects of several broadening gases on the absorption of radiation by methane at 7.65 μm and carbon dioxide at 4.3 μm and 14.8 μm. On the basis of their experiments at a single wavelength in each band, they concluded that the effects of a broadener would vary for different active gases and for different absorption bands of a single active gas. Following this was a paper published by Burch et al., (1962) which reported a very extensive study of the band averaged effects of several transparent gases on the absorption of infrared radiation by active gases in a number of absorption bands; among them was the 4.3 μm band of carbon dioxide. During the period from 1947 to 1962, a number of papers was published on the effects of broadening gases on the absorption spectra of nitrous oxide (Goody and Wormell, 1951), hydrogen chloride (Benedict et al., 1956 a & b ; Eaton and Thompson, 1959), and carbon monoxide (Benedict et al., 1961 ; Crane-Robinson and Thompson, 1962). Also during this period the study of the broadening ability of nitrogen on carbon dioxide spectra was being investigated (Howard et al., 1956; Edwards, 1960), and a book discussing spectral lines was published (Breene, 1961). By observing the high frequency wing of the 4.3 μm band of carbon dioxide, Winters et al., (1964) were able to infer the shape of the far wings of the collision

CHAPTER 2

THEORY

2.1 Introduction[1]

Theoretical and experimental studies of the absorption of electro-
magnetic radiation by materials have been conducted for many years.
These studies have resulted in the formulation of laws concerning the
transmission of radiation through the material, the discovery of
exceptions to these laws, and the development of several theories
which attempt to explain the empirical laws. In this chapter we will
examine the laws relevant to the experimental work which is discussed
later and to the broadening of absorption lines. The relative impor-
tance of several broadening mechanisms will be discussed and the
broadening source most important for measurements made in this work
identified. Finally, we will derive equations (based on a simplified
theory) that will allow us to draw certain conclusions from the mea-
surements made using a medium resolution infrared spectrophotometer.

2.2 Lambert's Law and Beer's Law

When a parallel beam of monochromatic radiation passes through a
medium, it may be observed that

$$I = I_o e^{-kl} \qquad (2.2.1)$$

[1] In addition to those specifically noted, references for this
chapter are Goody (1964), Gordy et al., (1953), Loeb (1961), Nielson
et. al., (1944), Townes and Schlawlow (1955) and Winters (1963).

where I = the intensity of the transmitted beam

I_o = the intensity of the incident beam

l = path length in the medium

k = absorption coefficient

This law, now generally called Lambert's Law, was discovered approximately 200 years ago. Roughly 100 years later A. v. Beer noted that the absorption coefficient, k, was often proportional to the concentration of the absorbing material. In a mixture of absorbers, Beer stated that the absorption coefficient was given by the expression

$$k = C_1E_1 + C_2E_2 + C_3E_3 + \ldots + C_nE_n \qquad (2.2.2.)$$

where C_1, C_2, C_3, . . . , C_n are the concentrations of the absorbing components and E_1, E_2, E_3, . . . , E_n are characteristic of the individual components and are called extinction coefficients. Lambert's Law is easily derived if one assumes that the change in intensity in a thin layer is proportional to the intensity of the beam incident on the layer and to the thickness of the layer. Beer's Law follows from the assumption that each molecule in the layer absorbs independently from every other molecule.

Deviations from Beer's Law were first observed for carbon dioxide in the infrared region by Ångstrom, (1893, 1901, 1908).
He constructed an absorption cell which was divided by a transparent partition into two equal halves, giving him two cells in series. One-half of the cell was filled with carbon dioxide while the other half was evacuated. The intensity of the infrared radiation passing through the cell was then measured. Next, a valve was opened between the two halves of the cell, allowing the carbon dioxide to fill the entire cell.

When the radiation passing through the cell was again measured, it was found that the intensity of the transmitted radiation had increased in apparent violation of Lambert's and Beer's Laws. When dry, carbon dioxide free air was admitted to the cell to increase the pressure to the original level, the absorption increased to the amount originally observed. On the basis of this experiment, Ångstrom concluded that the increased absorption was caused by pressure broadening of unresolved absorption lines or bands. This conclusion has since been shown to be correct. Since the time of Ångstrom, much theoretical and experimental effort has been expended in attempting to define the characteristics of the absorption lines and of the broadening mechanisms.

2.3 Line Broadening and Line Shapes

The sources of spectral line broadening that must be considered for carbon dioxide spectra in the infrared spectral region are:

1. Natural line broadening

2. Doppler effect

3. Pressure or collision broadening, i.e., disturbances caused by interaction between gas molecules

2.3.1 Natural Line Widths

The Heisenberg uncertainty principle shows that

$$\Delta E \Delta t \geq h/2\pi \qquad (2.3.1)$$

where ΔE is the energy spread in the excited state and Δt is the mean time the molecule spends in the excited state. The natural line width may be thought of as a disturbance of the molecule by zero point free space electromagnetic fields. For molecules having a permanent

electric dipole moment, a transition of frequency from an excited state to the ground state will give an absorption line of half width at half maximum of

$$\Delta f = \frac{32\pi^3 f^3}{3hc^3}|\mu|^2 \qquad (2.3.2)$$

where f = frequency

      h = Planck's constant

      c = speed of light = 3×10^{10} cm sec^{-1}

      $|\mu|$ = dipole moment in esu

For molecules like carbon dioxide which do not have a permanent dipole moment, the interaction between the molecule and the external field will take place through higher order moments, e.g., the quadrupole moment. The term $|\mu|^2$ in the above equation would then be replaced by terms in these higher order moments which have been neglected (because they are small with respect to the usual permanent dipole moment). We may still use the above equation to calculate an upper limit to the line width due to natural broadening for carbon dioxide by assuming some value of a fictitious dipole moment that may reasonably be expected to be large compared to the actually existing higher order moments. First, the equation is placed in a form more suitable to the units normally used in infrared spectroscopy. By means of the relations

$$\Delta f = c\Delta\nu \text{ and } \lambda = c/f$$

where λ = wavelength in cm and ν = wavenumber in cm^{-1} = $1/\lambda$ then

$$\Delta \nu = \alpha_N = \frac{32\pi^3\nu^3}{3hc}|\mu|^2 \qquad (2.3.3)$$

For a wavelength of $10\mu m$ and a dipole moment of 1 debye (10^{-18} esu), which is typical of a polar molecule such as ammonia, one finds that α is approximately 10^{-9} cm^{-1}. This is negligible in comparison with the minimum value of the half width observed in a planetary atmosphere, the minimum value being on the order of 10^{-3} cm^{-1}.

2.3.2 Doppler Broadening

The apparent shifting of the frequency of a beam of radiation caused by the motion of the molecules in the direction of propagation of the beam leads to a finite absorption line width. The apparent wave number shift is

$$\Delta \nu = \nu\left(\frac{V}{c}\right) \qquad (2.3.4)$$

where ν = the wave number of the radiation

and V = the velocity of the molecule in the direction of the beam. Assuming a Maxwelliam distribution of velocities, the probability that a molecule of a gas has a velocity, V, in a particular direction is proportional to

$$e^{-mV^2/2kT}$$

where m = molecular mass

k = Boltzmann's constant

T = absolute temperature

Then, the line intensity becomes

$$k_\nu = k_o\, e^{-\frac{mc^2}{2kT}\left(\frac{\nu-\nu_0}{\nu_0}\right)^2} \qquad (2.3.5)$$

where k_o = the absorption coefficient at the line center and ν_o = the wavenumber of the line center.

It can be seen that the line is symmetric about ν_o and has a half width at half maximum of

$$\alpha_D = \frac{\nu_o}{c}\sqrt{\frac{2kT}{m}\ln 2} = 3.581 \times 10^{-7}\sqrt{\frac{T}{M}}\,\nu_o \qquad (2.3.6)$$

where M is the molecular weight. Thus, for carbon dioxide at T = 300° K and a wavelength of 10 μm, the Doppler half width is appromimately equal to 10^{-3} cm^{-1}. This is negligible compared to the half width observed at atmospheric pressure (approximately 10^{-1} cm^{-1}). However, it is comparable to the observed half width at a pressure of 10^{-3} atmospheres, and consequently, Doppler broadening must be taken into account at low pressures.

2.3.3 Collision or Pressure Broadening

Natural and Doppler line widths have been shown to be small at gas pressures of the order of one atmosphere. It would then appear that pressure or collisional broadening will be the major source of the broadening of absorption lines at moderate pressures.

The study of the collisional broadening of spectral lines produced by the perturbing effects of other molecules was first studied by Michelson (1895). The work was continued by Lorentz, who published the results of a study (Lorentz, 1906) discussing the Lorentz line profile. He considered the molecules as a group of classical oscillators, each of which oscillates at constant amplitude, but is abruptly stopped after some time, t, where the number oscillating for time t, is given by $N_t = N_o\,e^{-t/\tau}$, where τ is the mean time between collisions. Upon restarting, the phase of the oscillation is assumed to be random

with respect to the phase at the time of the interruption. For a rotating molecule, this is equivalent to saying that the orientation is random. On the basis of the above assumptions, it is found that the absorption coefficient is of the form

$$k_f = \frac{S}{\pi} \left(\frac{\alpha_L}{(f - f_o)^2 + \alpha_L^2} \right) \qquad (2.3.7)$$

where S = a constant generally called the line strength

f_o = frequency of line center (natural frequency of the oscillators)

α_L = Lorentz half width at half maximum = $1/2\pi\tau$ (2.3.7a)

The Lorentz theory was extended by Van Vleck and Weisskopf (1945). They assumed that at the time that a radiating molecule undergoes a collision the phase following the collision is not random (as in the Lorentz model), but rather follows a Boltzmann distribution with respect to the electric field. Using a classical theory, a result is obtained that is somewhat similar to the Lorentz expression.

$$k_f = \frac{S}{\pi} \left(\frac{f}{f_o} \right)^2 \left(\frac{\alpha_L}{(f - f_o)^2 + \alpha_L^2} + \frac{\alpha_L}{(f + f_o)^2 + \alpha_L^2} \right) \qquad (2.3.8)$$

Since in the infrared region $\alpha_L \ll f_o$ the above expression reduces to the Lorentz profile in that region. If $\alpha_L \approx f_o$ as it may be in the microwave region, the second term introduces asymmetry into the profile. At high frequencies far from the line center, this profile would predict constant absorption. Many comparisons between experimental line shapes and the Van Vleck-Weisskopf shape have been made. At low pressures, the agreement is quite good in the microwave region,

however, the agreement deteriorates seriously at higher pressures.

Even if it were possible to develop line shapes of the type pre-viously discussed that were in agreement with experimentally deter-mined line shapes, the situation would still not be entirely satis-factory. It would be necessary to empirically fit certain parameters of the line shape, e.g., the half width or collision frequency (which is related to the half width) to match the data. One might think that the collision frequency could be obtained from kinetic theory. Unfortunately, however, results of attempts at this generally yield half widths that are consistently lower than observed absorption line half widths indicating that the kinetic collision cross section must be smaller than the optical collision cross section.

Several attempts at relating pressure or collisional broadening to the intermolecular forces have been made. The problem is so complex, however, that the theories developed are subject to many simplifying assumptions and, therefore, usually only apply under rather limited conditions. In general, the theories can be divided into two types, viz., impact theories and statistical theories. In impact theories, it is assumed that most of the time, a molecule is far enough from other molecules so that it may be considered free. Occasionally, however, it approaches another molecule closely enough that its energy levels are perturbed. During the encounter with this molecule, a transition may or may not occur. It is usually assumed that radiation takes place during the time that the molecule is free and that interruption takes place only during the brief and infrequent encounters. Statistical theories, on the other hand, assume that the

molecule is always under the influence of other molecules, although

the influence of the other molecules may be weak. The intensity of

the radiation at any frequency depends on the probability that the

molecule is perturbed enough by other molecules to make it radiate

at that frequency. Although either theory can, in principle, pro-

duce good results, both break down in practice when the simplifying

assumptions become unrealistic. The impact theories become inaccurate

at high pressures when the collisions are frequent and the radiation

during collisions becomes important while the statistical theories

produce good results only at low particle velocities.

The statistical method was introduced by Kuhn and London

(1934) and Kuhn (1934). Their analysis predicted a highly asymmetric

line shape. This shape has been observed at visible wavelengths.

Margenau (1949) developed a more sophisticated statistical theory

and applied it to the spectrum of ammonia. The theory predicted

half widths that were approximately correct and that varied in approxi-

mately the correct manner. Systematic variations between the theory

and experimental results do exist.

Collision theories for optical and infrared wavelengths

have been given by Lindholm (1945) and Foley (1946). The results of

their theory (which assumes no collision caused transitions) indicate

that for strong collisions, the line shape would be of the Lorentz

type. When weaker collisions were taken into account, however, it

was found that there was not only a broadening of the line about the

center frequency, but also a shift in the frequency of the line center.

The effect of the weak collisions was to decrease the center frequency.

The line shape produced was of the type

$$k_f = \frac{constant}{(f - f_o \pm a\alpha) + \alpha^2} \qquad (2.3.9)$$

It can be seen from this that the shift in center frequency is proportional to the line half width.

The most nearly complete impact theory to date has been developed by Anderson (1949). Although originally published for dipole-dipole interactions, the theory has been extended by Tsao and Curnutte (1962) to the case of dipole-quadrupole and quadrupole-quadrupole interactions. Based on the assumption that the relative motions of the particles are classical and that the time of collisions is small and allowing transitions to occur during collisions, Anderson determined the line shape to be as follows:

$$k_f = \frac{S}{\pi} \left(\frac{f}{f_o}\right)^2 \left(\frac{\alpha}{(f - f_o - a\alpha)^2 + \alpha^2} + \frac{\alpha}{(f + f_o + a\alpha)^2 + \alpha^2}\right) \qquad (2.3.10)$$

where S = a constant generally called the line strength

f_o = frequency of the line center

α = line half width at half maximum

It can be seen that this is similar to the Van Vleck-Weisskopf line shape except that the possibility of a center frequency shift is allowed. The theory predicts that this shift should be small for resonant self broadening and should be small in most other cases. These predictions have been verified experimentally. Line half widths, computed by means of Anderson's theory, have been determined for the self broadened spectrum of ammonia and the agreement is quite good. The results for foreign broadened ammonia spectra have been less satisfactory, although they are not too bad if the broadener has a

dipole moment not too different from the dipole moment of ammonia. Recently, attempts have been made to apply Anderson's theory to foreign broadened carbon dioxide spectra (Yamamoto, et al., 1968). The results of these calculations will be compared to our data in a later chapter.

In summary, it appears that the theory for the prediction of the spectra of pressure broadened gases is not yet complete. Even Anderson's theory, which is probably the best available, applies for the most part, near the line centers. The situation in the wings of lines where the force fields are more poorly known and possibly multiple collisions become more important (all of the impact theories discussed assume binary collisions) is even less well understood. In most of the work done in predicting spectra on the basis of known line positions, the line shape is being assumed and strengths and half widths empirically fitted. The line shape generally used in these calculations is the Lorentz profile at high pressures (typically $p > 0.1$ atmospheres) and a convolution of the Doppler and Lorentz profiles (called the Voigt profile) at lower pressures. The Voigt profile may either be read from precomputed tables or calculated directly, depending upon the problem to be solved and the facilities available. Methods of calculating the profile are discussed by Young (1965a), and precomputed tables of the profile have been presented by several persons including Posener (1959), Faddeeva and Terentev (1961), Fried and Conte (1961) and Young (1965b). A technique using empirically fitted line widths and calculated positions is described by Drayson and Young (1966) and Drayson, et al., (1968).

2.4 The Broadening Coefficient and Broadening Factor

In view of the present theoretical situation, we will proceed with the experimental work on the basis of a semiempirical set of relationships discussed below. The experimental data presented in succeeding chapters based on these relationships should be useful for the development of theories more sophisticated than that presented here. On the basis of assumed Lorentzian profiles, expressions will be developed for parameters (the broadening coefficient and the broadening factor) which will be a measure of the abilities of various infrared optically transparent gases for broadening carbon dioxide spectral lines.

As was noted in the discussion of the Lorentz theory, the half width of a Lorentz line is

$$\alpha_L = \frac{1}{2\pi\tau}$$

where τ is the mean time between collisions.

From kinetic theory, the collision frequency of an absorbing molecule, a, in a mixture with a broadening molecule, b, is (Chapman and Cowling, 1939)

$$\Gamma = 2\pi\left(\frac{2kT}{\pi}\right)^{1/2}\left\{ N_a(D_{aa})^2 \left(\frac{2}{M_a}\right)^{1/2} + N_b(D_{ab})^2 \left(\frac{M_a + M_b}{M_a M_b}\right)^{1/2} \right\}$$

(2.4.1)

where k = Boltzmann's constant

   T = absolute temperature

   D_{aa} = optical collision diameter for absorber with itself

   D_{ab} = optical collision diameter for collisions between absorber and broadener

N_a = number density of absorber

N_b = number density of broadener

M_a = molecular weight of the absorbing molecule

M_b = molecular weight of the broadening molecule

then

$$\alpha_L = \frac{\Gamma}{2\pi} = \left(\frac{2kT}{\pi}\right)^{1/2} \left\{ N_a (D_{aa})^2 \left(\frac{2}{M_a}\right)^{1/2} + N_b (D_{ab})^2 \left(\frac{M_a + M_b}{M_a M_b}\right) \right\}^{1/2}$$

$$(2.4.2)$$

substituting $\quad N_a = \frac{P_a}{kT}$ and $N_b = \frac{P_b}{kT}$

and letting

$$C_{aa} = (D_{aa})^2 \, (2/M_a)^{1/2} \qquad\qquad (2.4.2a)$$

$$C_{ab} = (D_{ab})^2 \, \left\{ (M_a + M_b)/(M_a M_b) \right\}^{1/2} \qquad (2.4.2b)$$

$$B = C_{aa}/C_{ab} \qquad\qquad (2.4.2c)$$

one finds

$$\alpha_L = \left(\frac{2}{\pi kT}\right)^{1/2} C_{ab} \, (P_b + BP_a) \qquad (2.4.3)$$

The quantity, B, will be referred to in this paper as the broadening coefficient. (In most papers it is referred to as the self-broadening coefficient). The quantity $(P_b + BP_a)$ is generally referred to as the equivalent pressure and is called that here. From the broadening coefficient, the ratio of the optical diameters can be readily determined by substituting Eq. (2.4.2a) and Eq. (2.4.2b) into

(Eq. (2.4.2c) and solving for the ratio of the collision diameters.

This yields
$$\frac{D_{aa}}{D_{ab}} = B^{\frac{1}{2}} \left(\frac{M_a + M_b}{2 M_b}\right)^{\frac{1}{4}}$$
(2.4.4)

It is sometimes desirable to determine the broadening ability of an optically transparent gas relative to the broadening ability of a second optically transparent gas; in some cases this improves the experimental-accuracy. In this case, nitrogen is generally used as the reference gas. A quantity named the broadening factor, F, is defined by

$$F_i = \frac{P_{N_2}}{P_i}$$
(2.4.5)

where P_{N_2} = nitrogen partial pressure to produce a given transmittance

P_i = partial pressure of i th gas required to produce on equal transmittance.

Depending upon the goals of the experiment and the available equipment both the broadening coefficient and the broadening factor may be determined as a function of wavelength or as band-averaged quantities. The broadening factor F_i, for a gas i, is related to the broadening coefficient for that gas and the broadening coefficient for nitrogen by the relationship

$$F_i = \frac{B_{N_2}}{B_i}$$
(2.4.6)

This can be shown to follow from the definitions of the broadening factor and broadening coefficient by writing Eq. (2.4.3) for

nitrogen and for the i th broadening gas. Assuming that equal
transmissivity implies equal line widths, the two expressions can
be equated and solved for P_{N_2}/P_i. The result will be equation
(2.4.6).

The broadening coefficient and broadening factor will differ
from gas to gas and will represent a measure of the line broadening
ability of each gas.

The equipment and techniques used for an experimental determina-
tion of the band-averaged broadening coefficient for nitrogen, band-
averaged broadening factors for argon, helium and oxygen, and wave-
length dependent broadening coefficients for argon, helium, nitrogen,
and oxygen will be discussed, along with the resulting measurements,
in succeeding chapters.

CHAPTER 3

EQUIPMENT

3.1 Spectrophotometer

The measurements were made using a Perkin Elmer Model 221 infrared
spectrophotometer equipped with a potassium bromide linear wave-
length prism interchange unit. This spectrophotometer is a double
beam optical nulling prism instrument of medium resolution (appromi-
mately 3 to 4 cm^{-1}) with an integral strip chart recorder which plots
transmissivity vs. wavelength. The optical nulling is achieved by
means of a servo driven filter. This filter (in which the trans-
missivity varies in a linear manner from 0 to 100% over the length
of the filter) is moved in the reference beam until the energy reach-
ing the detector through the reference beam equals the energy reach-
ing the detector through the sample beam. When the measured energy
of the two beams is equal, the position of the filter is measured
and interpreted in terms of the transmissivity of the sample beam.

The particular instrument used in these tests was modified as
follows: first, a precision wirewound potentiometer was added so
that an electrical analog of the transmissivity was available;
second, a cam and a minature switch were added to the wavelength in-
dicator output shaft so that an electrical pulse was generated at
intervals of 0.02 μm. During all tests the instrument volume was
purged with Liquid Carbonic Company "Hi Pure" grade nitrogen. A
photograph of the instrument with the long path gas cells installed
is shown in Figure 1.
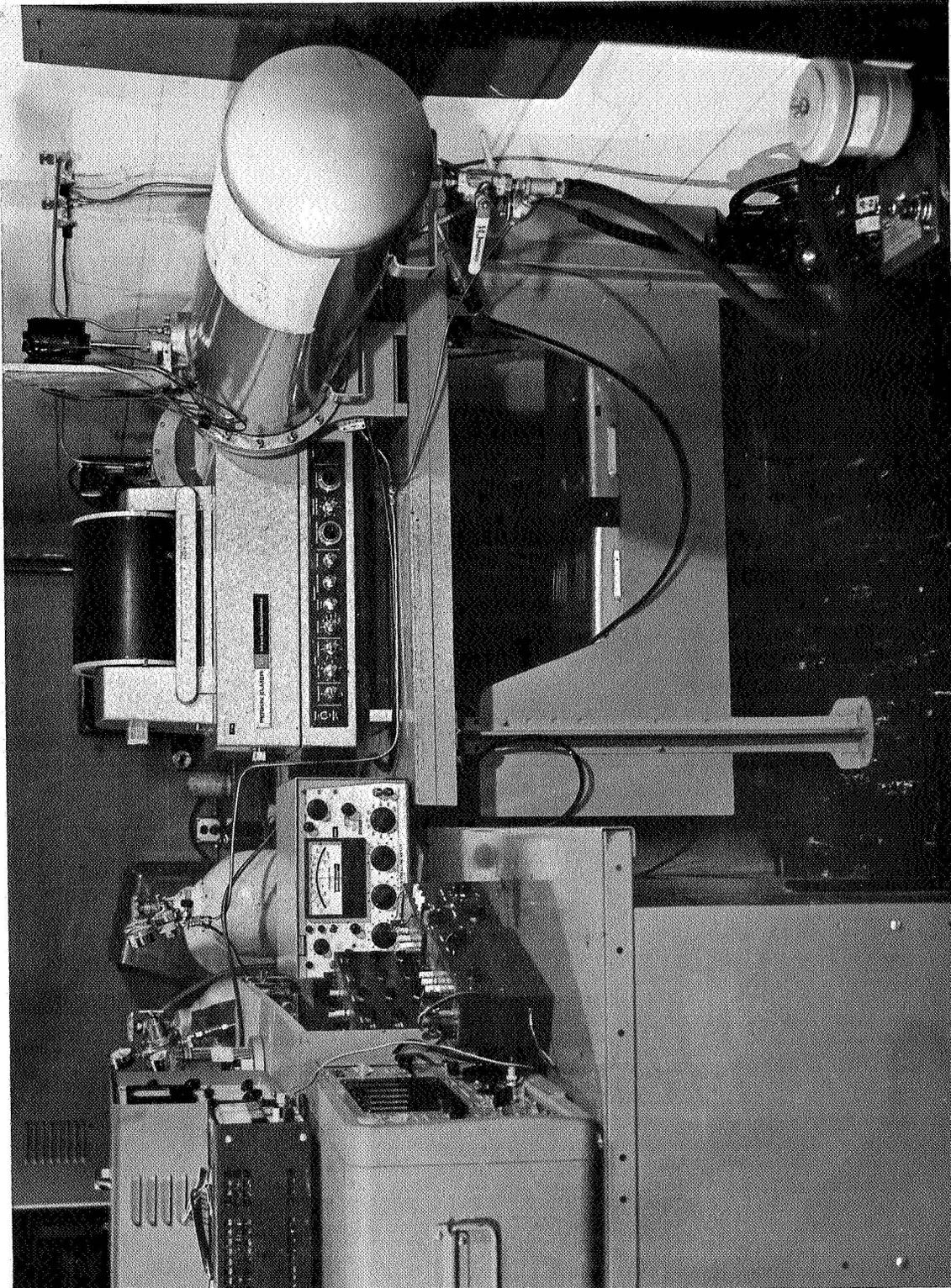
Figure 1.- Experimental apparatus.

The calibrations of both the wavelength scale and the trans-missivity scale of the instrument were checked. The wavelength scale of the instrument was calibrated by comparing the wavelength reading of the instrument with the known positions of the maxima of several CO_2 bands. It was found that the instrument read uniformly high by 0.05 μm. This correction was applied to all data during the data reduction.

Calibration of the transmissivity scale of the instrument proved to be more difficult. After a literature survey had yielded rela-tively little information on the testing of the linearity of spectro-photometer transmissivity scales, the following two different methods were tried.

In the first, the transmissivities of several different screens and perforated plates, placed in the sample beam, were measured. A number of difficulties arose using this method.

1. It was difficulty to find screens of different open areas. It seemed that most screens of usable mesh and wire sizes had transmissivities of approximately 40 to 60 percent.

2. The transmissivity was sensitive to the lateral location of of the screen in the beam. This was most pronounced for those screens having a rather coarse mesh and coarse wires.

3. Diffraction effects tended to defocus the instrument and thereby cause transmissivity readings different from the geo-metric transmissivity of the screen. This effect was most pro-nounced with some extremely fine mesh, etched screens.

4. The measured transmissivity tended to be wavelength sen-sitive. It is felt that this is not a result of instrument

linearity error since screens of different mesh sizes but of
similar transmissivity gave quite different results. This
was particularly troublesome at transmissivities between 0.3
and 0.75.

In spite of the foregoing difficulties, three screens were found
that gave satisfactory results when tested on this instrument and
on a factory calibrated Cary model 90 spectrophotometer at the
Goddard Space Flight Center of NASA. A photograph of these screens
(having transmissivities of 0.092, 0.158 and 0.861 as measured on
the Cary Instrument) is shown in Figure 2. The screen having the
highest transmissivity is a tungsten wire screen of the type used
in electron tube grids. The two screens of lower transmission are
of sheet metal having many small punched holes.

Since the transmissivity linearity calibration outlined above
was not particularly satisfactory, a second method of calibration
was tried. This method was suggested by Dr. Robert Howard (Howard,
1968) of the Perkin Elmer Corporation, and is the method used by the
Perkin Elmer Corporation for laboratory checks of instrument line-
arity. In this method, segmented disks are rotated at high speed
in the sample beam. If the ratio of open area to total area is
known and the rotation speed is selected so that synchronizing of
the external disk and the internal chopper does not occur, one
should be able to calibrate the transmissivity scale of the instru-
ment. Unfortunately, this method has certain weaknesses. The as-
sumption is made that the instrument electronics will treat a sig-
nal whose value is alternating rapidly between zero and one in the
same manner that it would treat a steady,
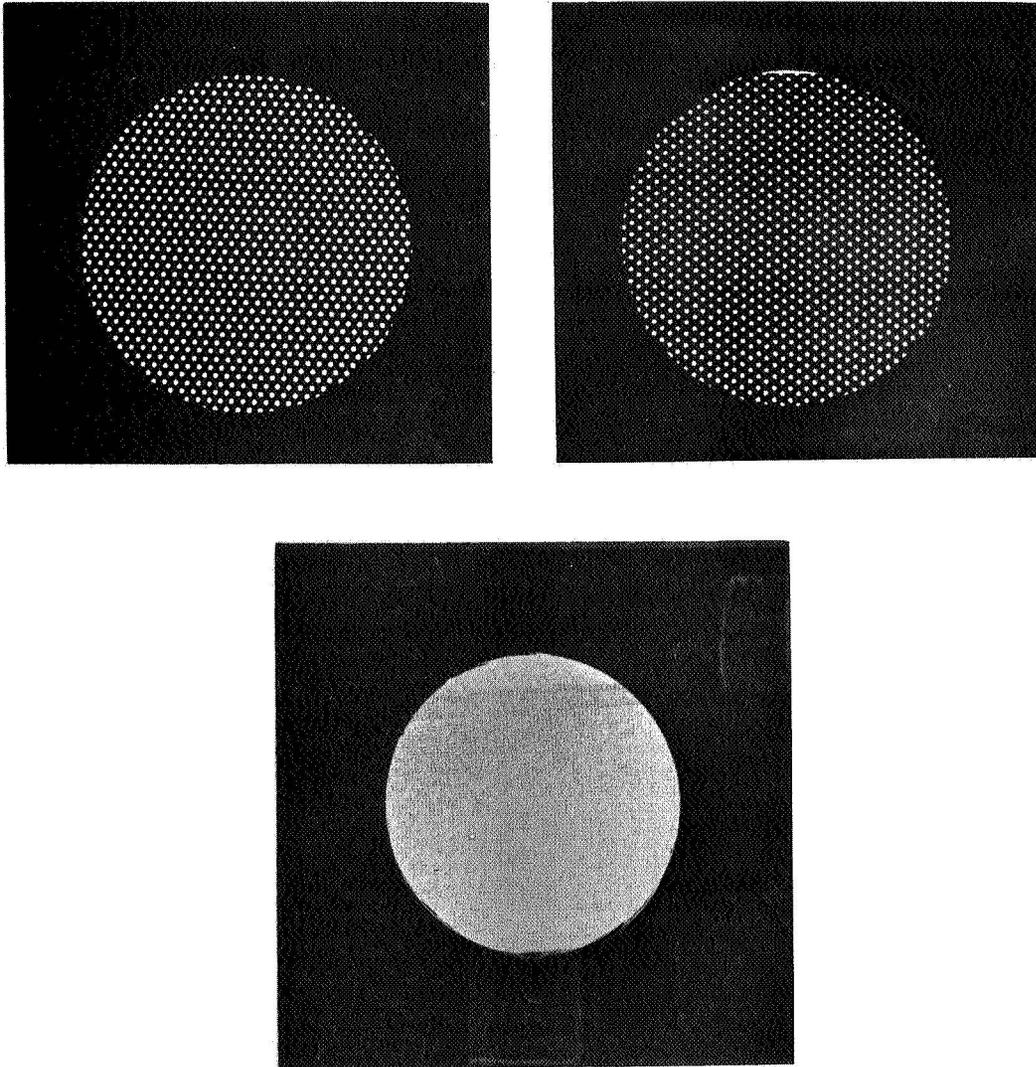
Figure 2.- Perforated screens used for spectrophotometer calibration.

gray signal where the transmissivity is equal to the ratio of chopper open area to chopper total area. As can be seen from Figure 3, the thermocouple detector has significant response at the chopping frequencies involved(by extrapolating the curve at 120 H$_z$)
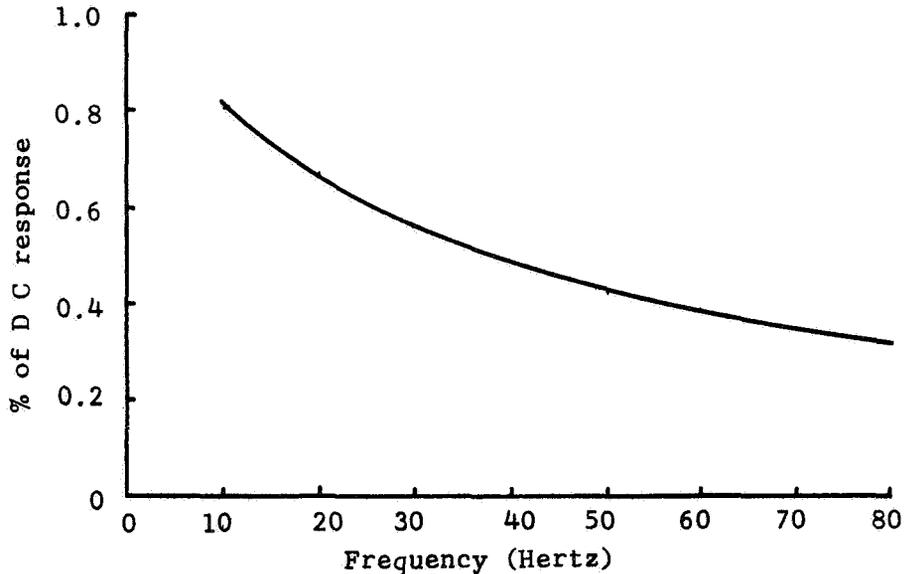
Figure 3. Thermocouple detector response curve.

As a result, the linearity of the thermocouple and the response of the electronics to high frequency inputs could become important (these, of course, are not important during the normal optical nulling operation of the instrument). Since the errors from these sources were thought to be small no attempt was made to correct the calibration for them.

To calibrate the instrument by this method a set of disks was made having open area to total area ratios of 0.05, 0.10, 0.20, 0.40, 0.60, 0.80, 0.90 and 0.95. A photograph of these disks is shown in Figure 4. The disks were rotated by a d.c. motor. The speed of the motor was approximately 3500 r.p.m. and was varied
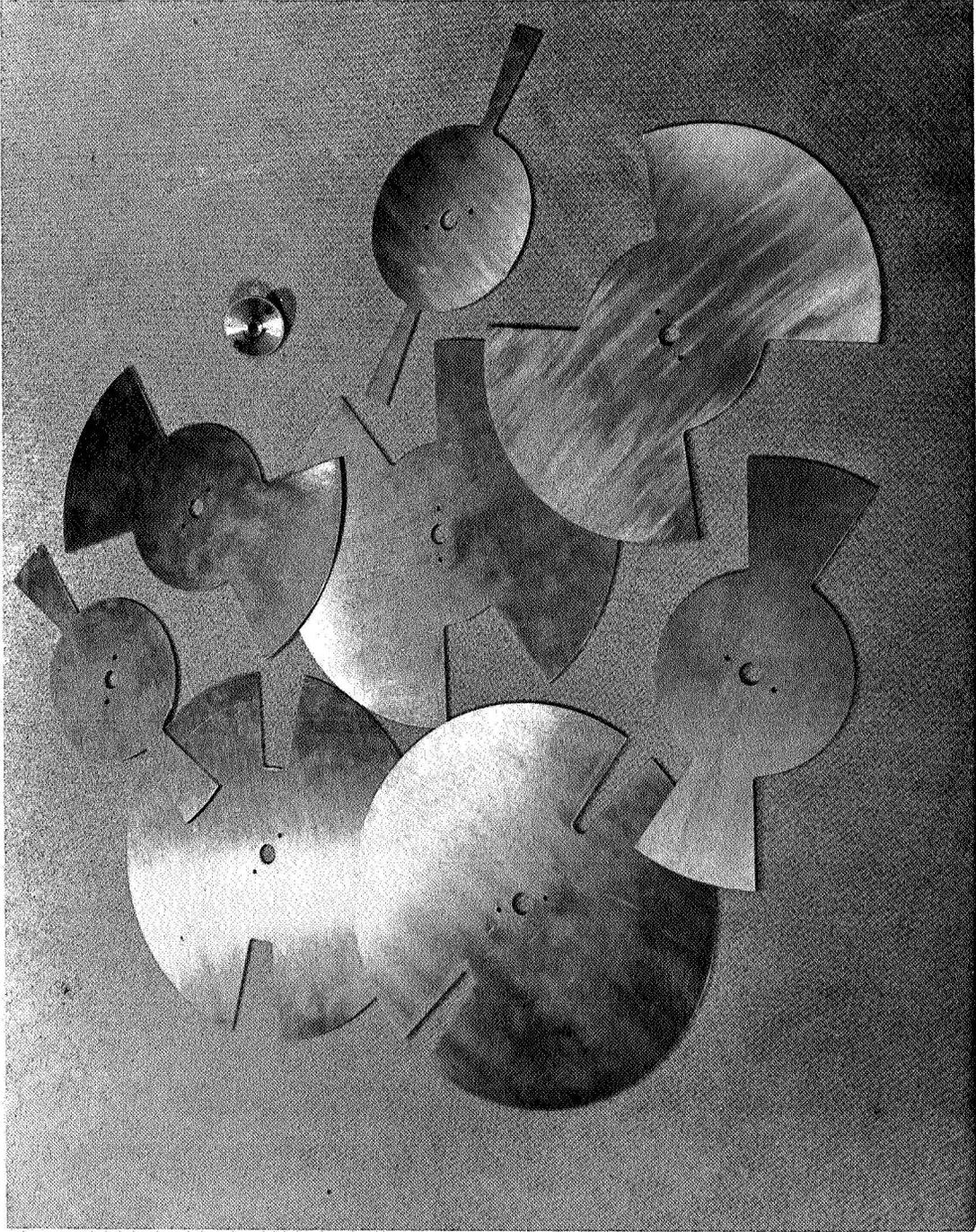
Figure 4.- Disks used for spectrophotometer calibration.

approximately 10% in the vicinity of this speed to insure that strobing with the chopper was not occurring.

The results of the two calibration methods are shown in Table 1. It would appear from the results obtained using the rotating disks that the instrument is more nearly linear than if judged on the basis of the results of the tests using the screens. It can be seen that the instrument linearity error was less than 1% in most cases.

Shortly after these linearity calibrations were completed, a more accurate method of measuring spectrophotometer linearity was discussed by Reule (1968). Reule's technique,called a supplementary light method, involves the addition, in several steps, of equal amounts of light. In principle, the method is the same as adding equal weights to a spring scale to determine its linearity. The implementation of the technique is rather complex, however, and for that reason it was not used here. The technique is best suited for the calibration of a master spectrophotometer against which other units can be checked.

3.2 Data Processing system

Since the spectrophotometer output was linear in wavelength (rather than linear in wavenumber) and because of a desire to correct the data for instrumental effects (zero shifts, non-linearities and scale factor changes) it was necessary to utilize a rather elaborate data processing system. A block diagram of this system is shown in Figure 5. The output of the spectrophotometer consisted of 0-5v analogue of the transmissivity $T(\lambda)$ while the wavelength output consisted of 3 volt pulses at wavelength increments of 0.02 μm.

29
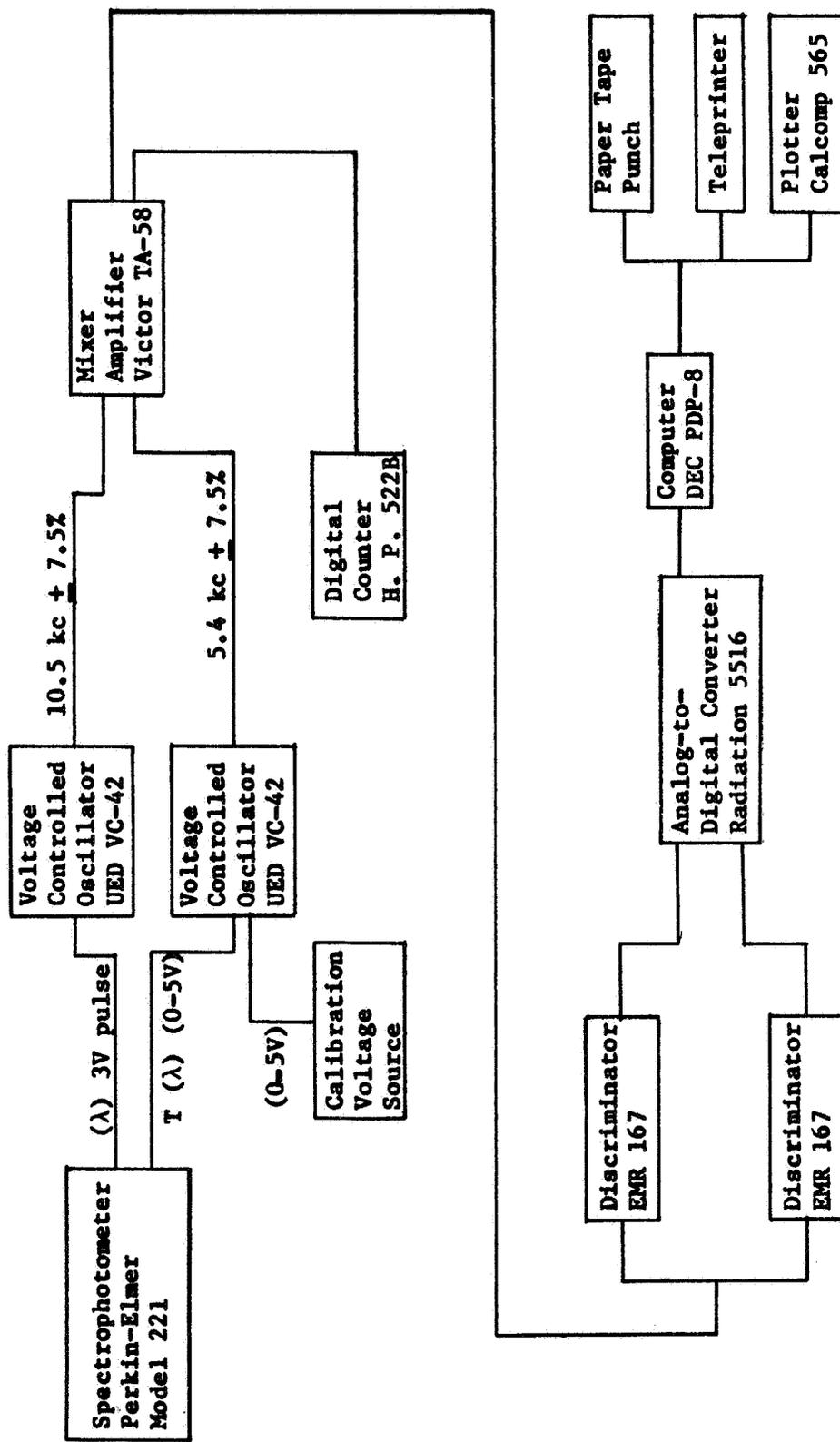
Figure 5. Block diagram of the data processing system.

These analogue outputs were converted to a frequency modulated A C

signal using the United Electrodynamics Corporation voltage con-

trolled oscillators. The oscillators had center frequencies of

5400 cps (T (λ)) and 10,500 cps (λ) and maximum deviations of

$\pm$ 7.5% of center frequency. The outputs of these oscillators

were mixed using a Victor Mfg. Co. TA 58 mixer amplifier. The

mixed, frequency modulated signal was then transmitted via shielded

cable to the High Altitude Engineering Laboratory Mobile Telemetry

Station which contained the remainder of the data processing system

(excluding the plotter which was located elsewhere). The fm signals

were converted to voltage analog   signals by the EMR discriminators

and fed to the Radiation Inc. A to D converter. The A to D con-

verter sampled the T(λ) signal at each command pulse from the read-

out of the instrument, i.e., every 0.02 μm. The twelve bit sample

of T(λ) was then stored in the PDP-8 memory for later processing,

and was typed also punched on paper tape as a permanent record. The

system was calibrated using the calibration voltage source (regulated

0,1,2,3,4,&5v) and the Hewlett Packard Model 522B digital counter.

The calibration procedure used will be discussed in detail in Chapter

4.

The calibration source consisted of a battery, two stage zener

diode regulator and voltage divider output network. This unit was

capable of producing highly stable, independently adjustable vol-

tages of 0.,1.,2.,3.,4., and 5. volts. Each voltage was adjustable

over a range of approximately $\pm$ 0.2v. The actual voltages were such

that the V.C.O. output frequency at each voltage was equal to the

V.C.O. output voltage at the corresponding transmissivity (as measured using the rotating disk) at a wavelength of 16 μm. Before and after each run, these six voltages were switched through the data system. The two sets of calibrations were averaged and the averaged values were assigned the transmissivity values of 0., 0.20, 0.40, 0.60, 0.80 and 1.00 by the computer. The data were then interpreted by linear interpolation between these points.

This data system proved to be highly reliable and stable over periods as long as several days. Over a period of thirty minutes (a run usually required less than twenty minutes) the calibrations would contain a 1σ error of less than 0.05%. It is estimated that the total error introduced into the transmissivity data by this system would have a 1σ value of less than 0.5%.

3.3 Pressure Gauge

All pressures were measured by means of an MKS Type 77 Baratron pressure gauge with 0 to 1000 Torr pressure sensing head. This is a highly sensitive diaphram type differential pressure gauge which senses the diaphram displacement by means of a differential capacitance A C bridge circuit. The pressure is read from four pressure readout dials which switch voltages to cause the bridge to become balanced. During these tests the "reference" side of the pressure gauge was maintained at a pressure of less than 10^{-3} Torr. This reference pressure was monitored by a NRC Thermocouple gauge. The Baratron pressure gauge can be seen in Figure 1.

The Baratron was initially calibrated by means of an air dead weight tester of very high repeatibility. The calibration was

TABLE I SPECTROPHOTOMETER LINEARITY CHECK
Perkin Elmer Model 221 Spectrophotometer
KBr Prism

$T_{Indicated}$	Wavelength μm.									T Average
	12	13	14	15	16	17	18	19	20	
.050	.052	.052	.052	.053	.053	.056	.057	.058	.058	.054
.092*	.081	.083	.083	.083	.082	.083	.082	.082	.082	.082
.100	.100	.102	.105	.108	.108	.110	.111	.111	.112	.107
.158*	.142	.143	.143	.142	.141	.141	.141	.141	.141	.142
.200	.202	.202	.203	.205	.207	.210	.211	.211	.212	.207
.400	.396	.397	.400	.403	.407	.408	.408	.409	.409	.404
.600	.598	.598	.600	.603	.606	.605	.608	.608	.608	.604
.800	.800	.800	.800	.806	.804	.802	.805	.806	.806	.803
.861*	.863	.862	.862	.861	.854	.851	.851	.851	.851	.856
.900	.898	.898	.900	.902	.899	.898	.900	.900	.901	.900
.950	.948	.947	.947	.950	.948	.945	.948	.946	.947	.947
1.053	1.062	1.068	1.065	1.075	1.062	1.050	1.052	1.052	1.056	1.060
1.111	1.130	1.130	1.123	1.130	1.119	1.112	1.105	1.105	1.107	1.118
1.250	1.268	1.270	1.268	1.273	1.262	1.245	1.247	1.247	1.250	1.259

* calibration points using screens

checked using a Pye Scientific Instruments precision cathatometer

to measure the height of the columns of either a butyl phthalate

or mercury manometer (depending on the pressure). The calibra-

tion using the air dead weight tester is shown in Table II.

TABLE II

BARATRON S/N1187

CALIBRATION DATA

PRESSURE P_x (Torr)	DECADE READING	ERROR $\pm$ (Torr)
0.00	0.00	0.00
15.51	15.51	0.00
23.27	23.28	+0.01
31.03	31.05	+0.02
77.57	77.60	+0.03
100.84	100.87	+0.03
201.69	201.85	+0.16
302.53	302.45	-0.08
403.37	403.35	-0.02
504.22	503.75	-0.47
605.06	604.15	-0.91
705.91	704.99	-0.92
775.72	774.80	-0.92
845.54	844.85	-0.69
1034.27	1037.00	+2.73

3.4 Gas handling system

The system for handling the sample gases consisted of con-

ventional regulators, valves, tubing and pumps. Since it was desir-

able to reduce the uncertainty in the sample composition to a mini-

mum, the following steps were taken:

1. All tubing carrying the sample gases was of stainless steel.

2. Needle valves controlling gas flow into the cells and the ball valves controlling the pumping of the cells were mounted directly to the cell body.

3. Provision for pumping all interconnecting supply tubing was arranged.

4. Pressure gauge volume and volume of connecting tubing was minimized. (In the worst case the tubing and gauge volume equalled three percent of the cell volume.)

In using this system the feed lines were pumped between sample changes and refilled with pure gas at a pressure greater than cell pressure. Needle valves were opened for a minimum time during filling to insure against back flow. The sample was then allowed to mix until the spectrum reached equilibrim.

3.5 Gas cells

Several gas cells of different lengths were used during the course of these tests. The two shorter cells were designed and built at the University of Michigan while the longer cells were commercial units.

The short cells (2.02, 8.74cm) were simple cylinders with provision for clamping the potassium bromide windows between O-rings at each end of the cell. A sketch of these cells is shown in Figure 6. Initially these cells were made of bare 6061-T6 aluminum. It was found, however, that this material would adsorb carbon dioxide for periods exceeding one half hour after filling. (This was ascer-
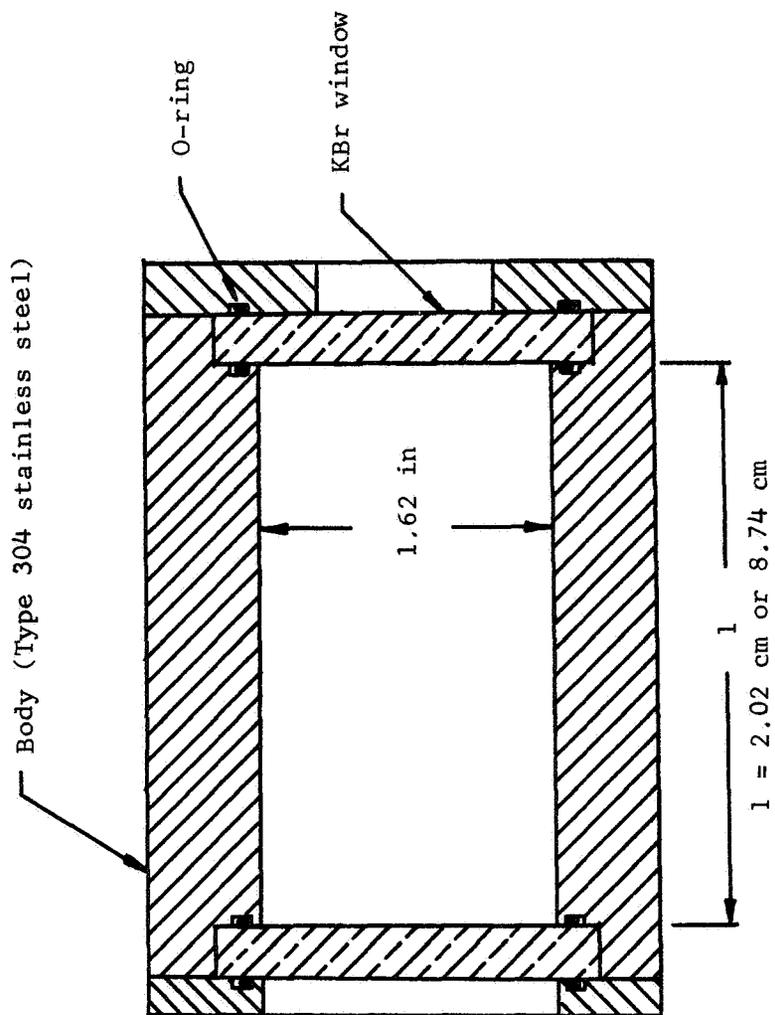
Figure 6. Drawing of the short path gas cells

tained by filling the cell with CO_2 and sealing it. Spectra were then run at regular intervals until no further change was noted.) It was also found that CO_2 desorption would continue for periods of the order of several hours after the cells were emptied of CO_2 and filled with nitrogen. (This was again ascertained by running spectra at regular intervals until equilibrium was reached.) After the cells were anodized it was found that the time to reach equilibrium during the adsorption process had been reduced to a few minutes, but that the time to reach equilibrium during the desorption process remained approximately the same as it had been for the bare metal. The amount of gas desorbed appeared to be approximately the same for an anodized cell as it had been for the same cell when bare. In view of the uncertainties that the adsorption and desorption would introduce in the composition of the gas sample, it was decided that another set of cells would be constructed of type 304 stainless steel. When these stainless steel cells were tested in a manner similar to that used for the aluminum cells, no desorption of CO_2 could be detected unless the cell was heated. Since all tests were conducted at room temperature, it was felt that the effect of desorption of carbon dioxide on sample composition could be neglected for tests using these cells. As a result of these tests, the stainless steel cells were used for all measurements involving cells of short length.

The longer cells were constructed of anodized aluminum by the Perkin Elmer corporation and were multiple pass cells. The one meter cells were fixed length four pass cells while the White-type

long path cells were adjustable in steps of four meters from four meters to forty meters. To speed the mixing of the gas mixtures a small, externally powered fan was installed in the long path sample cell.

Because of the problem of carbon dioxide desorption in the smaller cells discussed above, tests, similar to those previously described, were performed on the longer cells. On the basis of these tests it was decided that the CO_2 partial pressure of all sample gas mixtures would need to be greater than ten torr if the uncertainty in the sample composition were to be less than 1%. This condition was met in all subsequent measurements. A photograph of the long path cells installed on the instrument is shown in Figure 1.

CHAPTER 4

SPECTRA AND MEASURED EQUIVALENT WIDTHS

4.1 Introduction

As a check on instrument and data processing system operation, it was felt that it would be valuable to compare a few pure carbon dioxide and nitrogen broadened carbon dioxide spectra with previous experimental work and with the prediction of the analytical model of Drayson and Young (Drayson and Young, 1966 ; Drayson et al., 1968). Spectra were taken at two different path lengths, several pressures, and several carbon dioxide-to-nitrogen ratios. The test conditions were chosen to correspond to the experimental work of Burch et. al., (1962) and to the theoretical calculations previously reported by Drayson and Young (Drayson, et al., 1968)

4.2 Experimental Procedure

The data were obtained using the complete instrumentation system described in Chapter 3. The Perkin-Elmer Corporation long path cells were used at path lengths of 400 cm and 3,200 cm, with the path length of the reference cell matching the path length of the sample cell. The pressure in the reference cell (measured by a thermocouple gage) was maintained at less than 10^{-2} Torr. The optical path outside the cells was purged with nitrogen during all tests.

The spectra were obtained using the standard test procedure outlined below.

1. Evacuate the sample cell.

2. Set the spectrophotometer wavelength to 16 μm.

3. Block the sample beam.

4. Set the voltage controlled oscillator to the band-edge (as measured by Hewlett-Packard digital counter).

5. Open the sample beam.

6. Set the voltage controlled oscillator to the opposite band-edge.

7. Set the spectrophotometer wavelength to the beginning of the spectrum.

8. Fill the sample cell with gas to the desired pressure.

9. Operate the mixing fan.

10. Switch the spectrophotometer out of the data processing system and switch the calibrate box into the system.

11. Switch the calibration voltages through the system to the computer.

12. Switch the calibrate box out of the system and switch the spectrophotometer into the system.

13. Begin the scan.

14. Upon scan completion, again switch the calibration voltages to the computer.

Steps one through six of the above procedure were performed at the beginning of each data-taking session. The goal of this part of the procedure was to insure that the range of the six calibration voltages was the same as the range of the instrument output voltages. Steps seven through fourteen of the above procedure were performed in conjunction with each spectral scan.

During each scan the gas supply plumbing was evacuated. If the gas to be added to the cell were different from the gas last added to the cell, the supply plumbing was purged with the new gas at least twice during this evacuation process.

As is noted in step nine, mixing of the gas in the sample cell was insured by stirring the gases with a small fan mounted in the sample cell. This was operated for three periods of approximately 10 seconds each, with a waiting period between mixing of approximately 15 seconds. It had previously been found by running successive spectra that this mixing procedure would cause complete mixing.

4.3 Data Processing

Since the data existed in the form of a voltage analog of the transmissivity and an electrical pulse at 0.02 μm wavelength intervals, several operations were necessary to obtain final transmissivity and equivalent width data. The step-by-step procedure used was as follows

1. The calibration voltages were sampled by the analog-to-digital converter at the beginning of each run. Sixteen samples of each voltage were taken at 10-millisecond intervals. The 16 samples for each voltage were averaged and this average value was stored.

2. During the spectral scan, the voltage analog of the transmissivity was sampled whenever commanded by the wavelength voltage pulse. Upon being commanded, 16 samples (again at 10-millisecond intervals) were taken of the transmissivity data.

These 16 samples were averaged and the average value stored. At the scanning speed used, voltage pulses occurred approximately once every 2 seconds. As the transmissivity voltage was sampled, the averaged sampled value was typed out on the teleprinter and punched on paper tape.

   3. At the termination of the scan, the calibration voltages were again sampled. (Following the same procedure followed in step 1).

   4. The corresponding "before run" and "after run" calibration voltage samples were averaged and these averaged calibration voltages were stored. The "before run" samples, the "after run" samples, the average of the "before run" and "after run" samples, and the difference between overall averaged values of succeeding voltage steps were then printed out in octal form and were punched on paper tape. The paper tape containing these quantities, along with the transmissivity voltage samples constituted the permanent record of the raw data for that run. This completed the data sampling portion of the data processing. After the data for a particular run had been obtained and stored as outlined above, they were processed into "final" transmissivity data and the equivalent width calculated. The steps necessary to achieve this can be stated quite briefly.

   1. Determine the indicated transmissivity of the gas-sample cell combination from the data and calibrations.

   2. Correct for the transmissivity of the sample cell.

   3. Compute the equivalent width.

The detailed solution of the three parts of the above problem was

accomplished in the following way:

1. The computer was programmed to compare each stored voltage sample with the six double averaged calibration voltage samples and determine which adjacent pair of calibration samples bracketed the transmissivity sample. The computer then performed a linear interpolation between the calibration samples to determine the indicated transmissivity that corresponded to the stored voltage sample.

2. The correction for cell transmissivity is made by solving the equation

$$T_{gas} = \frac{T_{ind}}{T_{cell}} \qquad (4.3.1)$$

where T_{gas} is the transmissivity of the sample gas

T_{ind} is the instrument output

T_{cell} is the measured transmissivity of the sample cell relative to the transmissivity of the particular reference cell in place at the time. T_{cell} would be more precisely defined as

$$T_{cell} = \frac{T_{sample\ cell}}{T_{reference\ cell}} \qquad (4.3.2)$$

T_{cell} was stored as a table in the computer. This table was loaded by measuring the transmissivity of the sample cell while evacuated and storing the indicated transmissivities in the T_{cell} table. After dividing the indicated transmissivity by the cell transmissivity, the computer stored the computed gas transmissivities.

3. Before calculating the equivalent width of the spectrum in units of cm^{-1} (the standard unit of measure of equivalent width)

it is necessary that the absolute value of the wavelength of each
transmissivity sample be determined. At this point, we know only
that they are spaced at 0.02 μm intervals. The wavelength of the
data points was established by inspecting the transmissivity
values of a CO_2 spectrum having a maximum absorption of appromi-
mately 0.25. The sharp absorption band (the main Q branch) near
the band center was examined and the data point having the minimum
transmissivity value was assigned the wavelength of 14.99 μm. It
was found that the wavelength calibration of the system was very
stable, not varying by more than $\pm$0.01 μm over 8 hours.

After the wavelength of the transmissivity samples had been
established, the computer calculated the integral of the trans-
missivity vs. wavenumber spectrum in units of cm^{-1}. This was per-
formed using a trapezoidal rule integration scheme. The wave
number increments between samples had been calculated and stored
in the computer in tabular form. Upon completion of the compu-
tations, the wavelength and transmissivity of each sample and the
value of the integral of transmissivity over the wave number range
of the spectrum were printed out. This completed the processing
of the data by the data processing system.

It would seem that this should complete the processing of
the data. (Except for subtracting the computed transmissivity
integral from the quantity (ν_{max} - ν_{min}) to determine the
equivalent width of the spectrum). Unfortunately, this was not
found to be the case; the system displayed two effects for which
further correction of the data was required. These were scale

factor change and zero shifts. It could be seen by examination of the instrument strip chart record that the scale factor change was occurring in the instrument itself. The scale factor variation from run to run was small, approximately 0.5%, and apparently random. Examination of both the instrument strip chart record and the computer output of spectra that were opaque over some region near the band center indicated that the zero shift was a combination of apparently random instrument shifts, approximately 0.2%, and a slow drift in the instrumentation system occurring as a result of a change in the output voltage of a bias battery. It appeared that the battery voltage drifted rather rapidly initially (for the first half hour after turn-on) then very slowly for the remainder of the day. The offset in the data as a result of both effects was generally less than 1 percent.

The corrections for the two above effects were applied as follows:

1. From each transmissivity value was subtracted the signed average of the instrument output for 50 data points in a region where the transmissivity value was known to be zero. (If no such points existed for a particular spectrum, another spectrum containing such points was run immediately following the running of the spectrum to be corrected).

2. The transmissivities for the first 10 points and the last 10 points of the spectrum were averaged (the spectrum was always started and ended outside the 15 μm band), and all transmissivities (after the above zero shift correction was applied) were divided

by this average value.

To correct the computer-calculated transmissivity integral, the product of the signed zero offset and the interval of the calculation, i.e., Z_{off} ($\nu_{max} - \nu_{min}$) was subtracted from the computer output. This result was then divided by the scale factor of the spectrum (the averaged value of the first 10 and the last 10 data points). Since this represented the last correction to the data, the computed value of the transmissivity integral was subtracted from the interval over which the spectrum was measured and the equivalent width determined, i.e.,

$$A = \int_{\nu_{min}}^{\nu_{max}} A_\nu \, d\nu = \int_{\nu_{min}}^{\nu_{max}} (1 - T_\nu) \, d\nu = \int_{\nu_{min}}^{\nu_{max}} d\nu - \int_{\nu_{min}}^{\nu_{max}} T_\nu \, d\nu$$

$$= (\nu_{max} - \nu_{min}) - \int_{\nu_{min}}^{\nu_{max}} T_\nu \, d\nu \tag{4.3.3}$$

4.4 Data Accuracy

The accuracy of the data is influenced by errors from many sources. Some of the error sources are:

1. Errors in the knowledge of sample characteristics; presure, temperature, composition, and path length

2. Instrument errors; scale factor changes, nonlinearity, zero shift, and wavelength calibration

3. Errors in the data transmission system; nonlinearity, zero shift, scale factor changes, and digitizing errors

4. Data processing errors; round off and integration errors.

If these errors are viewed as being random with respect to each other (although they may be systematic in the sense that they will occur repeatedly under the same test conditions) they can be combined to obtain the standard deviation of the total error. This was done using the calibration curves for the various instrument parameters wherever available, data from other sources (previous calibrations of the data system on the bus, for example) and, where all else failed, educated guesses. It appears from this analysis that the transmissivity data have a 1σ error of approximately 1 percent while the equivalent width data have a 1σ error of approximately 3 percent at $A = 30$ cm^{-1} decreasing to approximately 1.5 percent at $A = 100$ cm^{-1}.

4.5 Results

The test conditions, the measured equivalent widths and the equivalent widths measured by Burch, et al., (1962) and calculated by Drayson, et al., (1968) for similar test conditions are shown in table III. The theoretical calculations used a mixed Doppler-Lorentz line shape with variable line half width. This model is discussed in detail in Drayson and Young, (1966), and Drayson, et al., (1968). It can be seen that the agreement between our equivalent width data and the data of Burch, et al is very good, disagreeing at most by 4 percent. Since the accuracy claimed by Burch, et al., for their data is only ±5 percent, and since our data are estimated to have a 1σ error of 3 percent both sets of data are essentially in agreement. The agreement between our experimental data and the predictions of the model of Drayson and

TABLE III

COMPARISON OF MEASURED

AND CALCULATED EQUIVALENT WIDTHS

P_{CO_2} (Torr)	l (cm)	w (atm cm)	P_{N_2} (Torr)	T (°C)	This Work	$\overline{A}$ (cm^{-1}) (Drayson et al 1968)	(Burch et al 1963)
12	400	6.32	0	25	35.8	33.3	34.6
12	400	6.32	751.4	25	95.8	97.	95.3
24	400	12.63	0	25	59.3	N.A.	58.3
24	400	12.63	736.	25	113.	115.7	113.
100	400	52.63	0	25	122.	N.A.	121.
100	400	52.63	0	25	122.	N.A.	121.
25	3,200	105.26	0	25	114.	N.A.	110.
25	3,200	105.26	771.3	25	164.	174.2	164.
50	3,200	210.53	0	25	144.	143.6	143.
50	3,200	210.53	689.2	25	179.	194.7	183.

Note: The two values at l = 400 cm, P_{CO_2} = 100 Torr are for two different samples.

N.A. Theoretical equivalent widths not available.

Young are within the experimental accuracy except for conditions of relatively low amounts of carbon dioxide when broadened by approximately one atmosphere of nitrogen at long path lengths. Under these conditions, the model predicts an equivalent width approximately 6 to 8 percent higher than was measured.

In Figure 7 are shown three spectra selected from those summarized in table III. It can be seen that the agreement between the two sets of experimental data is good when one allows for the somewhat higher resolution of this work as compared to the work of Burch. The comparison with the theoretical model is also good (within the experimental error for the two spectra (Figure 7 (a) and 7(b)) for pure CO_2 samples . The agreement between the experimental spectrum and the theoretical calculations deteriorates for carbon dioxide broadened by a relatively large amount of nitrogen (Figure 7 (c)). The disagreement is particularly pronounced in the regions from 595 to 615 cm^{-1}, from 710 to 740 cm^{-1} and also in the wings of the band. The disagreement between the model and experiment under these conditions has been noted previously (Drayson et al., 1968). It might be possible that the strength of some of the bands may have been incorrectly estimated. This seems a particularly appealing possibility in the regions from 595 to 615 cm^{-1} and from 710 to 740 cm^{-1}. The discrepancy between the predicted transmissivity in the wing region of the band might be due to a change in line shape since in this spectrum the absorption lines are broadened as a result of carbon dioxide-nitrogen collisions rather than as a result of carbon dioxide-carbon dioxide collisions
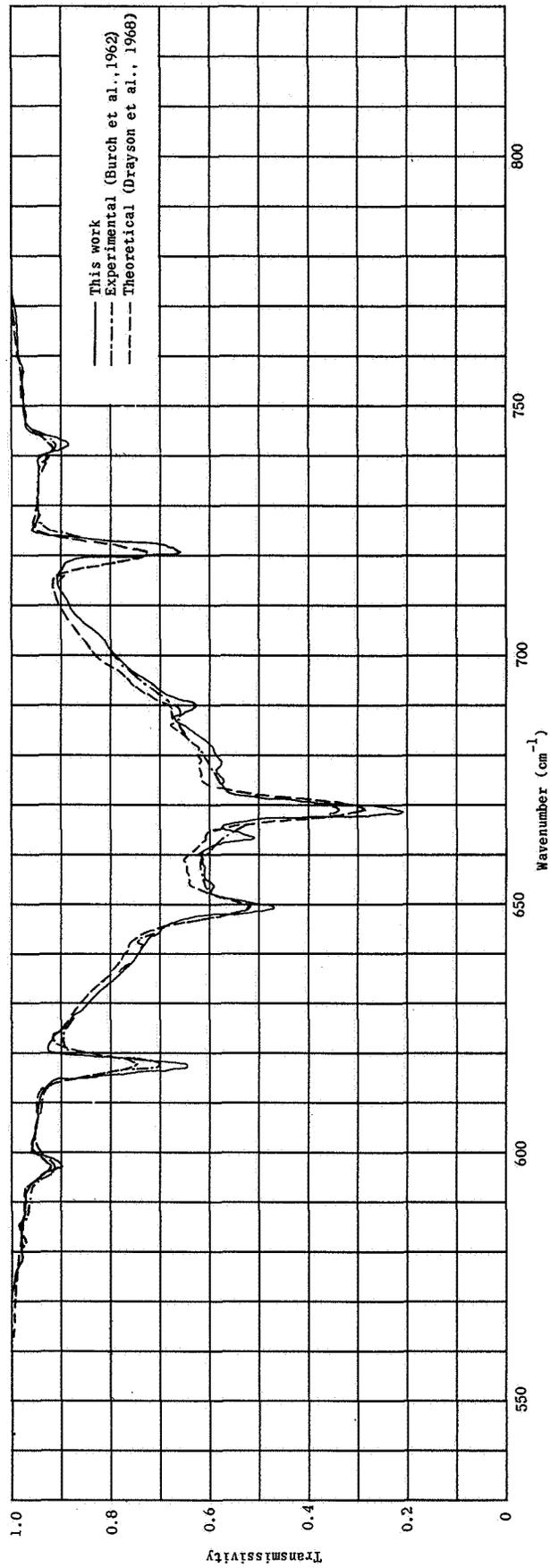
(a) $P_{CO_2} = 12$ Torr, $l = 400$ cm.

Figure 7.- Comparison of spectra with other experimental results and with theoretical predictions.
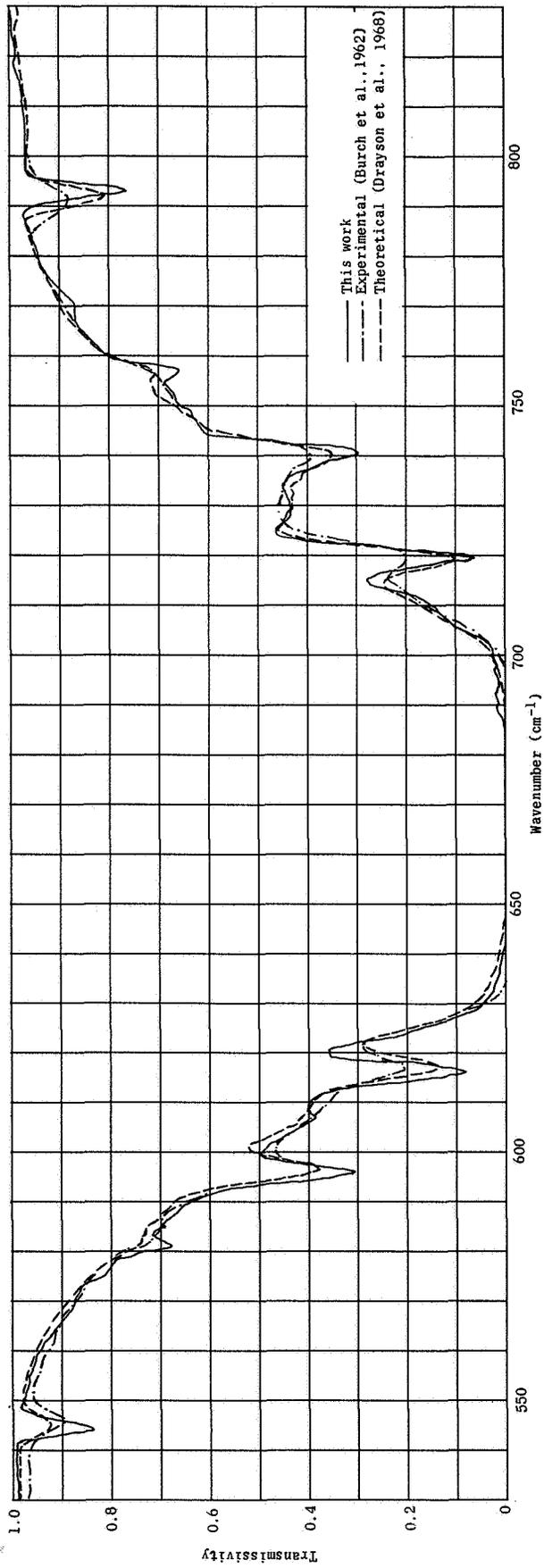
(b) P_{CO_2} = 50 Torr, l = 3,200 cm.

Figure 7.- Continued.
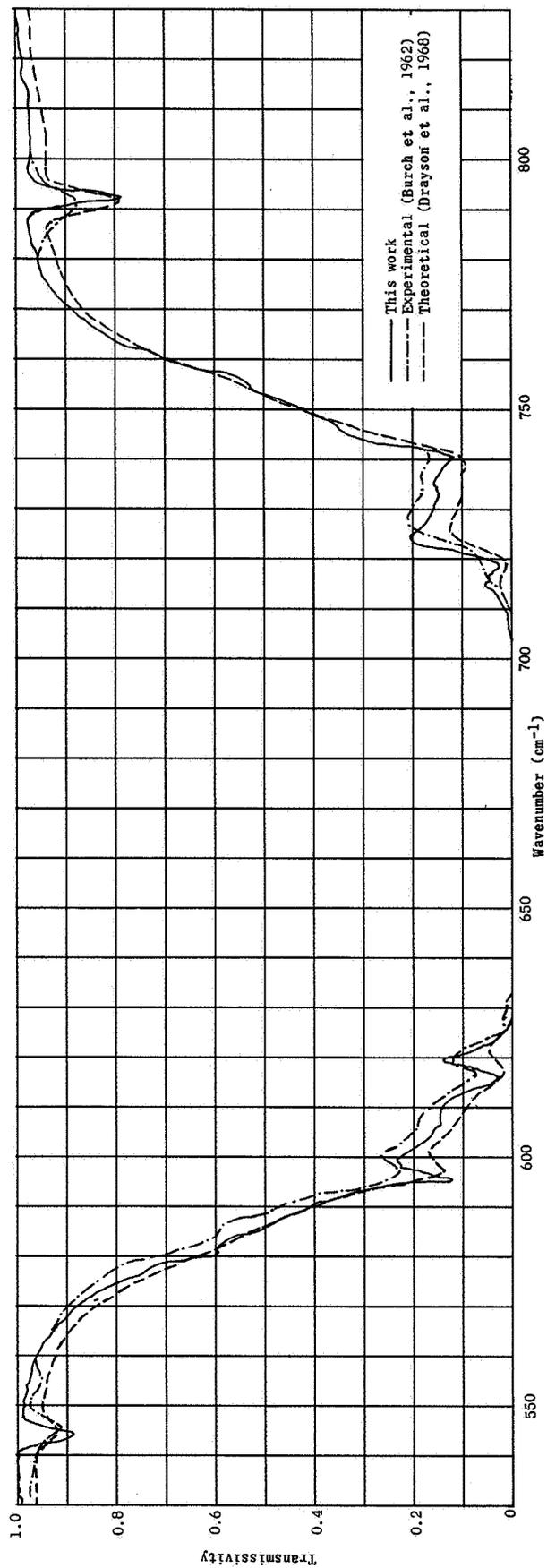
(c) P_{CO_2} = 25 Torr, P_{N_2} = 771.3 Torr, l = 3,200 cm.

Figure 7.- Concluded.

as in the two previously discussed spectra. This possibility will be discussed later in this report in connection with other data that will be presented. The data presented here are neither of the proper type nor of sufficient quantity to draw any definite conclusions concerning the difficulties of the theoretical calculations.

It would appear then from the above data that the instrument and data processing system and the methods of processing the data are capable of producing spectra and equivalent width data that are in agreement with the work of others.

CHAPTER 5

BAND-AVERAGED BROADENING COEFFICIENT FOR CO_2

5.1 Experimental Method

The self-broadening coefficient, B, for carbon dioxide relative to nitrogen has previously been determined by estimation from curves of B (ν) vs. ν in the 15 μm band (Burch, et al., 1962), by measuring the broadening of individual absorption lines in the 10.6 μm-band using a laser source (Patty, et al., 1968) and by a method using cells of different lengths in the 4.6 μm-band (Anderson, et al., (1967). In general, the values obtained for the different methods have been consistently equal to approximately 1.3. Uncertainties claimed range from ±0.03 in the work of Anderson, et al., (1967) to ±0.08 in the case of Burch, et al., (1962).

In this study, a band-averaged value of B has been determined at one optical mass using the third method mentioned above. The method consists essentially of comparing the amount of radiation absorbed by an equal amount of carbon dioxide while being broadened by both nitrogen and carbon dioxide in one case and carbon dioxide alone in another case. For the measurement of the effect of carbon dioxide-carbon dioxide broadening, one fills a cell (hereafter called the short cell) with carbon dioxide at some partial pressure $P^S_{CO_2}$ and measures the equivalent width of the spectrum obtained. The effective pressure in this cell is $P^S_e = B_{avg}P^S{CO_2}$. To examine the effect of carbon dioxide-nitrogen broadening, one fills a longer cell with the same optical mass of carbon dioxide as was contained in the short cell. The partial pressure in this cell is $P^L_{CO_2}$.

Nitrogen is now added to this cell. The effective pressure in this cell is $P_e = B_{avg}P_{CO_2}^L + P_{N_2}$. The nitrogen partial pressure is increased in steps and the equivalent width determined at each step. A plot of equivalent width versus total pressure is then made. At that nitrogen pressure at which the equivalent width of the spectrum of the carbon dioxide - nitrogen mixture is equal to the equivalent width of the spectrum of pure carbon dioxide, the equivalent pressure in the two cells are equal (this follows from Eq. (2.4.3) and the assumption that equal equivalent widths implies equal line widths) and one can write the equation

$$B_{avg}P_{CO_2}^S = B_{avg}P_{CO_2}^L + P_{N_2} = P_e \qquad (5.1.1)$$

where $P_{CO_2}^S$ = carbon dioxide pressure in the short cell

$P_{CO_2}^L$ = carbon dioxide partial pressure in the long cell

P_{N_2} = nitrogen partial pressure in the long cell

or solving for B_{avg}

$$B_{avg} = \frac{P_{N_2}}{P_{CO_2}^S - P_{CO_2}^L} \qquad (5.1.2)$$

Using this equation one can then determine B_{avg} if the carbon dioxide pressures in the two cells and the nitrogen pressure necessary to cause the same total absorption in the two cells are known.

5.2 Instrumentation and Data Processing

The instrumentation used for the measurements was the complete system described in Chapter 3. The methods used for obtaining and

processing the data were described in 4.2 and 4.3.

5.3 Test Conditions

The Perkin-Elmer long path cells were set at 400 cm (the "short" cell) and at 1,600 cm (the "long" cell). The carbon dioxide partial pressure was 100 Torr in the short cell and 25 Torr in the long cell. The nitrogen partial pressure was varied from zero to 412 Torr. A summary of the test conditions is presented in Table IV.

5.4 Results

The measured equivalent widths for the various samples are listed in Table IV. Figure 8 is a plot of measured equivalent width versus total pressure in the 1,600 cm cell (the "long" cell). Taking 121.85 as the average value of the equivalent width determined for the two 100 Torr pure carbon dioxide samples in the 400 cm cell, it is found that this value of equivalent width would be achieved at a nitrogen partial pressure of 98 Torr in the long cell. Substituting this value and the appropriate values for the carbon dioxide partial pressures in equation (5.1.2), we find that the value of B_{avg} is

$$B_{avg} = \frac{P_{N_2}}{P_{CO_2}^S - P_{CO_2}^L} = \frac{98}{100 - 25} = 1.30$$

5.5 Accuracy

It can be seen by examining figure 8 that the nitrogen partial pressure (and hence the value of B) at which equality of equivalent widths appears to be achieved is extremely sensitive to small errors in the determination of the equivalent width of either sample. It
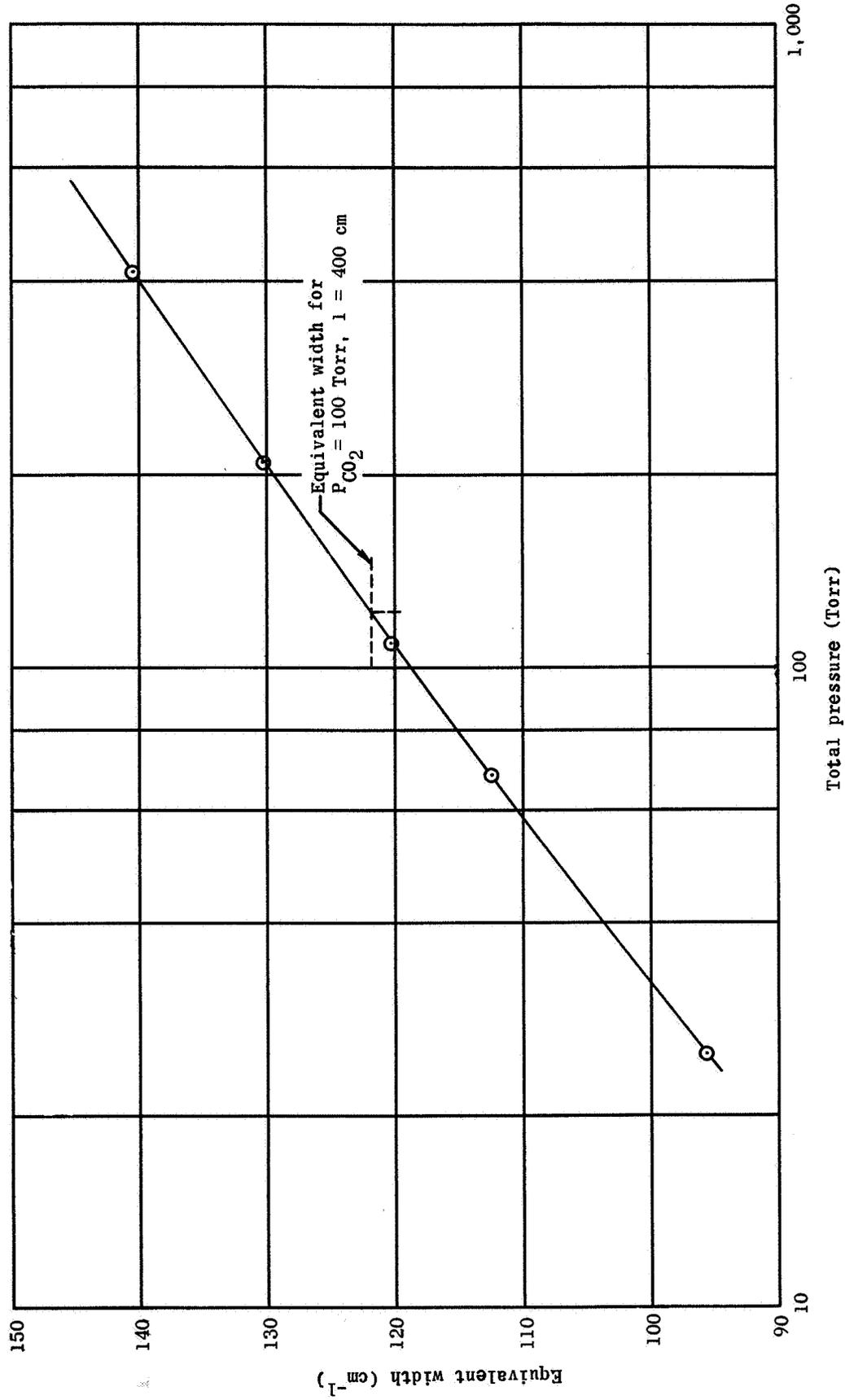
Figure 8.- Equivalent width vs. total pressure, $P_{CO_2} = 25$ Torr, $l = 1,600$ cm.

is rather insensitive, however, to errors in the equivalent width determination if the errors for both samples are of similar magnitude and in the same direction. An attempt was made to achieve this equality of errors by taking the data after the system had been operating for several hours, by taking the data in as short a time as possible and by using only those data for which the corrections were small.

A second source of error is the problem of achieving equal optical masses in the two cells. Since the optical mass (for these uniform paths) is the product of the path length and the carbon dioxide partial pressure, the problem really concerns the accuracy with which one can measure the pressure and the path length. As can be seen from the calibration of the Baratron pressure gauge, the accuracy of the pressure measurement is quite high, approximately 0.1%. It is rather difficult, however, to measure the exact path length traversed by the beam in the long path cells, but path length is probably accurate to better than ± 0.25 percent.

In view of the difficulties outlined, it is estimated that a reasonable value of the 1σ error in the value of B is approximately 0.08. It is doubtful if greater accuracy than this could be achieved with the experimental technique and instrumentation system used for the measurements discussed here.

5.6 Discussion of Results

Table V displays B values obtained by other researchers, and it can be seen that most of the values are between 1.2 and 1.4. The results of this study (1.30) agree well with those values. When one

considers these data it should be noted that

1. The values of B are for different bands

2. Some of the values are for the broadening of individual lines near their centers (the laser method) while others are for averages over an entire band.

3. These data are quite uncertain (probably more uncertain than most experimenters admit).

In view of the above, it is felt that the agreement among the various workers is unusually good.

TABLE IV

TEST CONDITIONS AND MEASURED EQUIVALENT WIDTHS USED

FOR THE DETERMINATION OF THE BROADENING COEFFICIENT FOR NITROGEN

P_{CO_2} (Torr)	l (cm)	$\bar{w}$ (atm cm)	P_{N_2} (Torr)	T (°C)	A (cm^{-1})
100	400	52.63	0	25	121.76
100	400	52.63	0	25	121.95
25	1600	52.63	0	25	95.8
25	1600	52.63	43.	25	112.6
25	1600	52.63	84.1	25	120.2
25	1600	52.63	184.	25	130.2
25	1600	52.63	412.	25	140.4

TABLE V

EXPERIMENTAL BROADENING COEFFICIENTS FOR NITROGEN

Band or Wavelength	Investigator	Type of Measurement	B
15μm region (667cm^{-1})	This work	Band average	1.30 $\pm$ 0.08
10.4μm (961cm^{-1})	Patty et al.,(1968)	Laser, P(20) line	1.33 $\pm$ 0.05
10.4μm (961cm^{-1})	McCubbin and Mooney (1968)	Laser, P(20) line	1.37
2.8μm (3620cm^{-1})	Burch et al., (1968)	Near line centers	1.21 $\pm$ 0.09
2.8μm (3620cm^{-1})	Burch et al., (1968)	In line wings	1.30
4.3μm (2350cm^{-1})	Anderson et al., (1967)	Band average	1.30 $\pm$ 0.03
2.06μm (4853cm^{-1})	Vasilevskii et al., (1967)	High resolution spectroscopy	1.49 to 2.13
10.4μm (961cm^{-1})	Boutin et al., (1967)	Laser, P(20) line	1.12 $\pm$ 0.07
10.4μm (961cm^{-1})	Rosetti et al., (1967)	Laser, P(20) line	2.04 $\pm$ 0.34
15μm (495 to 875cm^{-1})	Burch et al., (1962a)	Mean of B (ν)	1.30 $\pm$ 0.08

TABLE V (CONCLUDED)

Band or Wavelength	Investigator	Type of Measurement	$\underline{B}$
2.76μm(3713.2cm⁻¹) 4.3μm(2350cm⁻¹) 9.6μm(1063.1cm⁻¹) 10.4μm(961.3cm⁻¹) 15μm(667.3cm⁻¹) }	Edwards (1960)	Band average	$(2 + 0.5\ P_{CO_2})^{CO_2}$ P_{CO_2} in atm.
Same as Edwards (1960)	Howard et al., (1956)	Band average	2
4.3μm & 14.8μm	Coggeshall and Saier (1947)	Single wavelength	1.25

CHAPTER 6

BAND-AVERAGED BROADENING FACTORS FOR ARGON, HELIUM, AND OXYGEN

6.1 Introduction

The ability of a gas to broaden the spectral lines in an absorp-
tion band is usually expressed relative to the broadening ability
of another gas. The reference gas may be either the absorber itself,
in which case the quantity determined is similar to the broadening
coefficient of Chapter 5, or it may be some other gas. When the
second method of expression is chosen, the reference gas normally
used (at least in studying carbon dioxide infrared absorption spectra)
is nitrogen. The result is then usually expressed in terms of the
broadening factor as defined in Eq. (2.4.5). The abilities of argon,
helium, and oxygen relative to the ability of nitrogen to broaden
carbon dioxide spectra have been determined. These data are pre-
sented and discussed in this chapter.

6.2 Experimental method

In this part of the investigation the broadening abilities of
argon, helium, and oxygen relative to that of nitrogen are discussed.
The ability of each gas to broaden the spectral lines is expressed
as a band-averaged broadening factor, F, as defined in Eq. (2.45)

$$F_i = \frac{P_{N_2}}{P_i}$$

where P_i = the pressure of the ith gas required to produce a
specified equivalent width for some CO_2 sample

and P_{N_2} = the nitrogen pressure required to produce the same
equivalent width for an identical CO_2 sample

61

In practice, the relative broadening factor is determined by plotting equivalent width as a function of gas pressure for each broadening gas. It is then possible to read from the plot the pressure of each broadening gas that corresponds to any given equivalent width. The relative broadening factor for each gas can then be readily determined.

The major advantage of this method (as compared to a technique that results in a broadening coefficient similar to that measured for nitrogen in Chapter 5) is that accurate data are more easily obtained. In the method discussed in Chapter 5 it is necessary to place the same optical mass of carbon dioxide in two cells of different lengths with no readily available means, independent of pressure and cell length measurements, of determining the amount of carbon dioxide in the cell. In determining broadening factors relative to nitrogen, one has only to check the equivalent widths of the spectra for the pure carbon dioxide samples. If the carbon dioxide samples are consistent, it is then only necessary for good accuracy that the pressure gauge be repeatable and reasonably accurate.

6.3 Instrumentation and Data Processing

The system used for obtaining the measurements discussed in this chapter was the complete set up described in Chapter 3. The experimental procedure followed was described in section 4.2 with one exception. Since no mixing fan was installed in the small cells (8.74 and 100 cm) used here, it was necessary to wait approximately 25 minutes after filling the cells to be sure the gases were mixed.

This time period had been found to be sufficient for complete mixing by taking several spectra of the same sample at various time intervals after filling. The rather long time period was required to allow the small amount of gas in the pressure gauge and connecting tubing to mix with the gas in the cell.

The data processing techniques were described in section 4.3 except that the cell transmissivity table was loaded somewhat differently. In these tests, the table was hand-loaded into the computer. The values loaded were the average of approximately five cell transmissivity runs. This was an attempt to reduce the effects of noise. It was feasible because the transmissivity of these cells was highly stable, while the transmissivity of the long-path cells changed each time the path length was changed.

6.4 Test Conditions

Spectra were obtained for path lengths of 8.74 and 100 cm. Carbon dioxide partial pressures were 100 Torr in the 8.74 cm cell and 30 and 100 Torr in the 100 cm cell. Broadening gas pressures varied from zero to 700 Torr in the case of the 30 Torr carbon dioxide samples and from zero to 620 Torr in the case of the samples having a carbon dioxide partial pressure of 100 Torr. Broadening gases were argon, helium, nitrogen, and oxygen. The test conditions describing each sample are listed in Table VI. All the spectra for any one carbon dioxide partial pressure-path length combination were obtained during a single test session.

6.5 Results

The measured equivalent widths for the various spectra are

shown in Table VI. The equivalent widths are plotted as a function
of total gas pressure in Figure 9. Several equivalent widths were
selected for each figure and the corresponding gas pressures deter-
mined from the curves. The equivalent widths selected, the cor-
responding gas pressures, and the calculated broadening factors
relative to nitrogen are shown in Table VII. The broadening factors
were averaged over each optical mass and were also averaged overall
for each gas. These averages are also presented in Table VII.

6.6 Accuracy

As has been noted earlier, the accuracy of the relative broad-
ening factors is controlled primarily by the repeatability of the
instrumentation and data processing system; the absolute accuracy
of the system is of lesser importance. For example, it can easily
be shown that a systematic five percent shift in the values of the
equivalent width would change the relative broadening factors by
only one percent.

Some measure of system repeatability (including the experimenter,
a variable often overlooked and whose properties are difficult to
measure) can be obtained by comparing the measured equivalent widths
of the four spectra of pure carbon dioxide at each optical mass. It
can be seen that the scatter in the measured equivalent width for
each of the three sets of four independently formed samples is very
small, the 1σ scatter being only 0.17 percent. Because of the repea-
tability of the system, the accuracy of the pressure gauge, and
the insensitivity of the broadening factors to systematic errors,
the broadening factors derived here are felt to be considerably

TABLE VI

TEST CONDITIONS AND EQUIVALENT WIDTHS

FOR THE BAND AVERAGED BROADENING STUDY

P_{CO_2} (Torr)	w (atm cm.)	l (cm.)	Broadening Gas	P_B (Torr)	T (°C)	A (cm^{-1})
100	1.153	8.74	N_2	0	32	33.56
				120.4		39.93
				320.12		45.90
				620.		51.33
			O_2	0.		33.51
				120.		39.18
				324.26		44.54
				620.		49.61
			He	0.		33.66
				120.		38.75
				321.4		44.34
				619.92		49.10
			A	0		33.55
				120.		38.89
				323.3		44.23
				620.		49.19
30.	3.95	100	N_2	0		39.08
				9.30		42.01
				60.36		52.62
				200.16		65.97
				702.		81.86
			O_2	0		38.83
				60.		50.60
				200.		63.95
				700.5		79.69
			He	0		38.99

TABLE VI (CONCLUDED)

P_{CO_2} (Torr)	w (atm cm.)	l (cm.)	Broadening Gas	P_B (Torr)	T (°C)	A (cm^{-1})
30.	3.95	100	He	60.1	32	50.38
				201.		62.95
				702.		78.46
			A	0		38.92
				60.1		49.98
				200.1		62.61
				700.		78.36
100	13.16		N_2	0.		84.62
				124.34		96.43
				320		105.63
				620		112.04
			O_2	0		84.75
				120.18		95.10
				320.18		103.79
				623.68		110.34
			He	0		84.78
				120.52		94.65
				320.05		103.22
				620.15		109.61
			A	0		84.71
				120.3		94.53
				320.6		102.97
				619.6		109.35
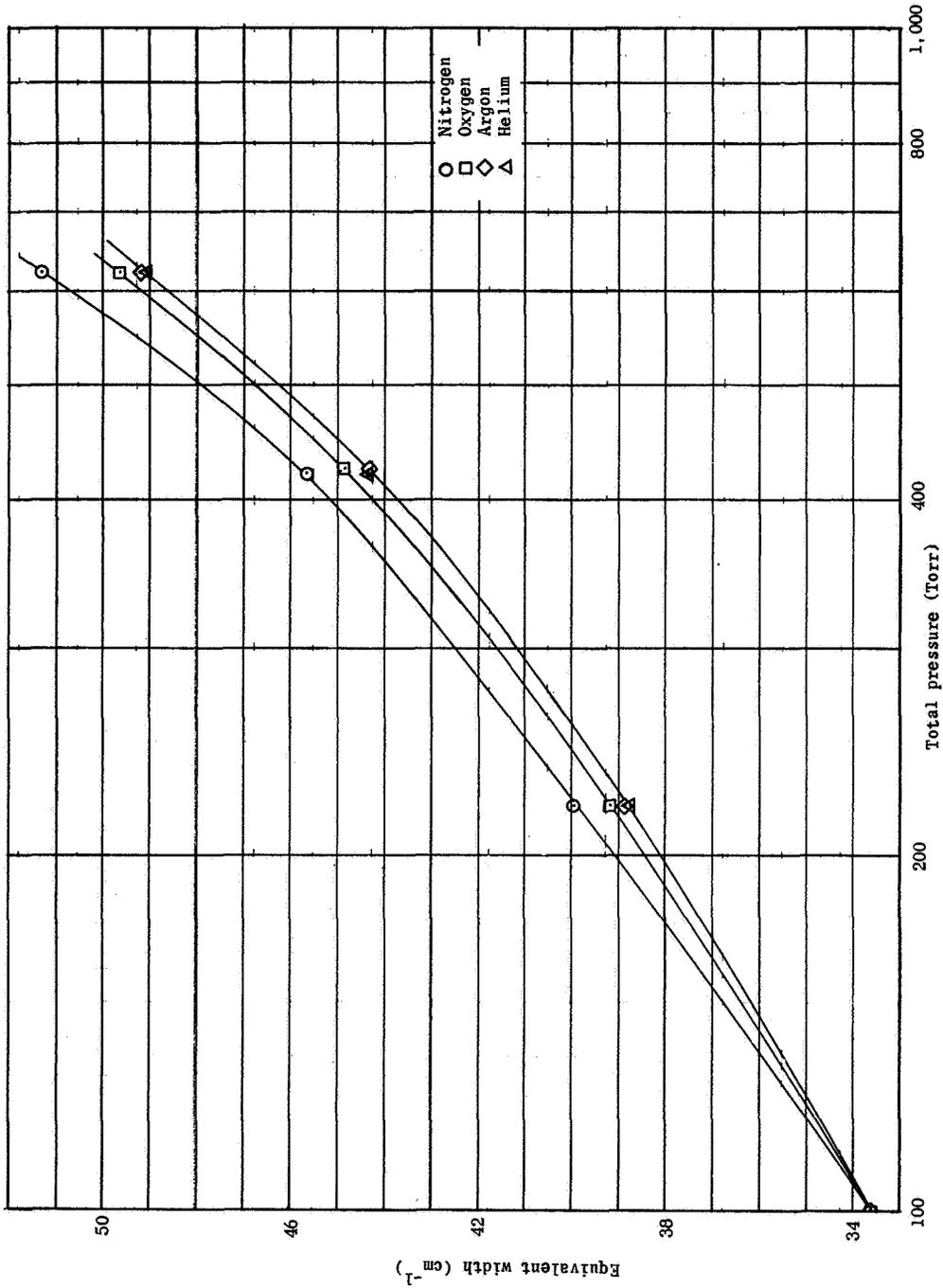
(a) P_{CO_2} = 100 Torr, l = 8.74 cm.

Figure 9.- Equivalent width vs. total pressure for various broadening gases.
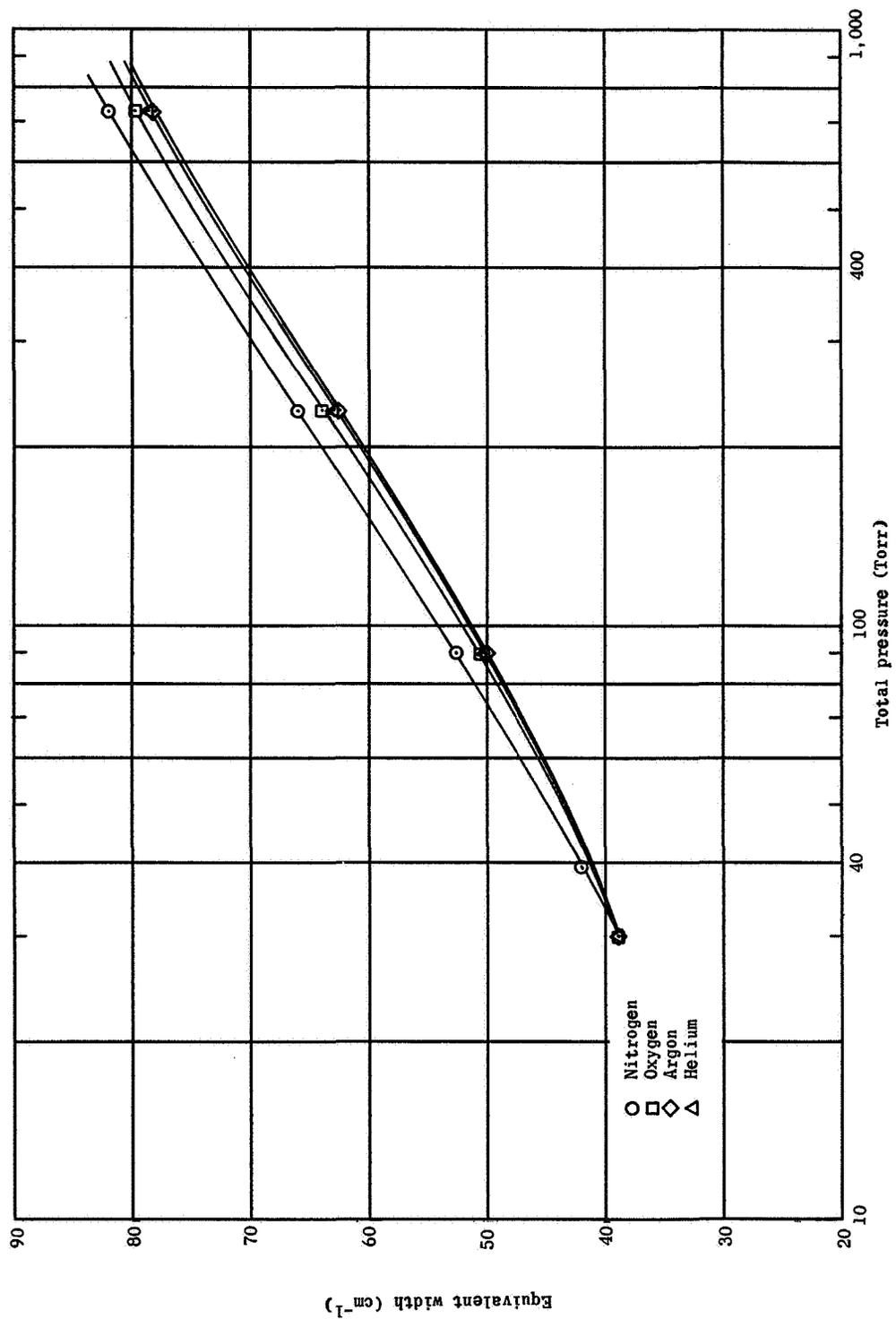
(b) P_{CO_2} = 30 Torr, l = 100 cm.

Figure 9.- Continued.
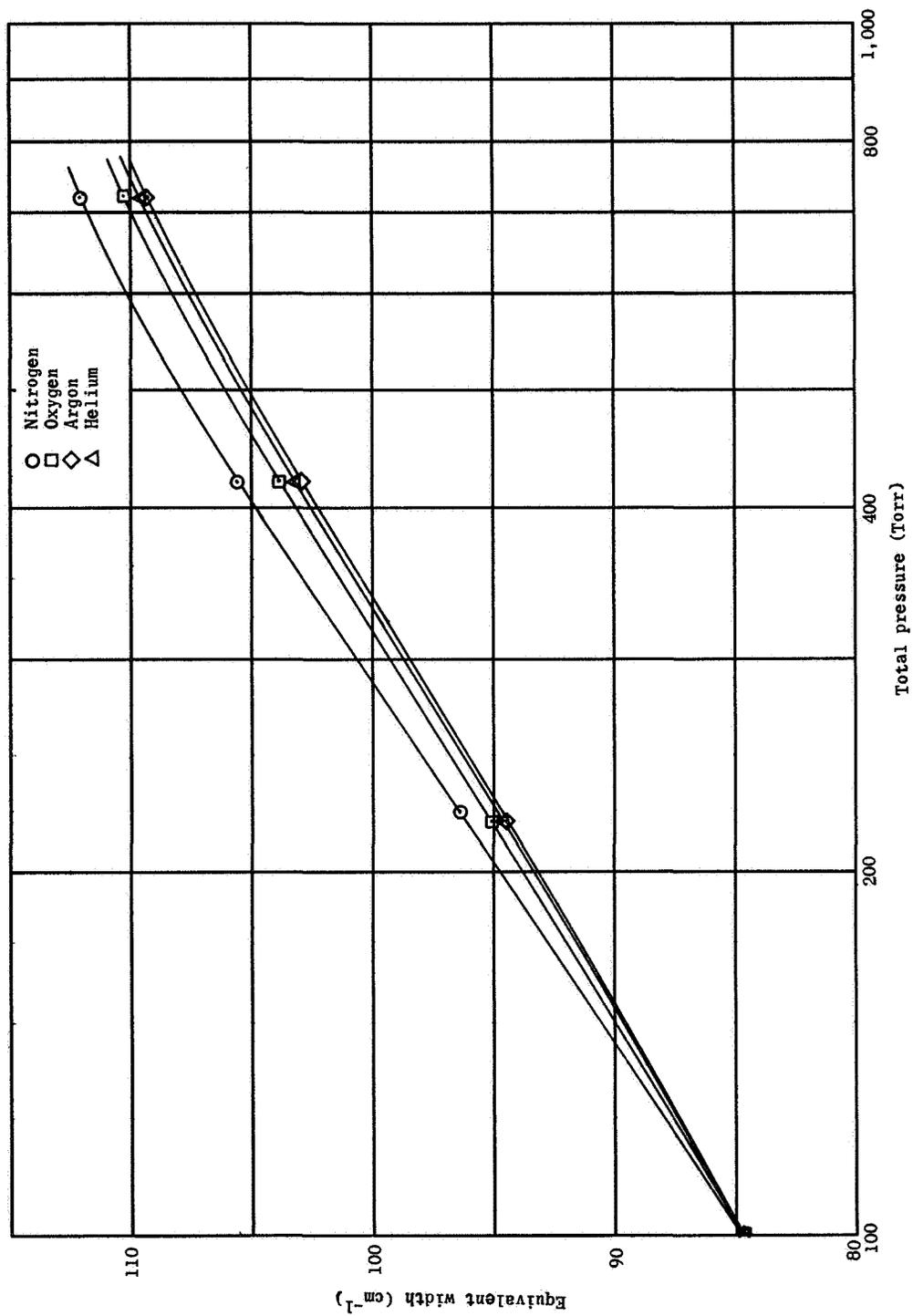
(c) $P_{CO_2} = 100$ Torr, $l = 100$ cm.

Figure 9.- Concluded.

more accurate than the corresponding coefficient for nitrogen that was determined in Chapter 5 of this work. It is estimated that the 1σ error in the relative broadening factors is probably no greater than 0.02 and that it is very unlikely that the order of broadening ability (exygen, helium, and argon) is incorrect.

6.7 Discussion of Results

Presented in Table VII are the broadening factors for argon, helium, and oxygen relative to nitrogen. Values of the broadening factor were calculated for at least three values of the equivalent width for each of the three optical masses. The values of the broadening factor for all of the equivalent widths were averaged over each optical mass and were also averaged over all equivalent widths and optical masses; this value is shown as the overall average.

It will be noted that the deviations of the average values from the overall average are rather small being no greater than five percent. Within each optical mass the factor varies somewhat with equivalent width. This variation is small in the case of the two larger optical masses and is within the data scatter. In the case of the smallest optical mass, however, the variation is larger, the value of the broadening factor tending to increase with increasing equivalent width. There is no obvious explanation for this from these data but this point will be discussed further in the next chapter when the wavelength dependence of the broadening coefficients is discussed.

The broadening factors have not been previously determined in

TABLE VII

SUMMARY OF THE BAND AVERAGED BROADENING FACTOR CALCULATIONS

P_{CO_2} (Torr)	w (atm cm)	l (cm)	A (cm⁻¹)	P_{N_2} (Torr)	P_{O_2} (Torr)	P_A (Torr)	P_{He} (Torr)	F_{O_2}	F_A	F_{He}
100	1.153	8.75	40.	123.	144.	157	157	0.85	.78	.78
			43.	218.	250.	270	270	.87	.81	.81
			46.	332.	369.	388	388	.90	.86	.86
			49.	438.	492.	515	515	.89	.85	.85
						Average		.88	.88	.83
30	3.95	100	60.	122.	147.	162.	156.	.83	.75	.78
			70.	273.	323.	365.	357.	.85	.75	.77
			80.	600.	730.	823	800.	.82	.73	.75
						Average		.83	.74	.77
100	13.16	100	95.	103.	118.	130.	127.	.87	.79	.81
			100	187.	217.	238.	231.	.86	.79	.81
			105.	305.	360.	395.	383.	.85	.77	.80
						Average		.86	.78	.81
					Overall Average			.85	.78	.80

the 15 μm region for carbon dioxide, but there have been investi-
gations in which these factors (or data from which relative broad-
ening factors can be derived) have been determined in other carbon
dioxide absorption bands. Table VIII displays the relative broad-
ening factors for several carbon dioxide absorption bands measured
by other workers. Also shown in this table are the overall average
values of the broadening factors from Table VII.

The data shown for the 4.3 μm (2,350 cm^{-1}) band
obtained by Burch et al., (1962a) were determined by the same
method as that used in this work. The carbon dioxide partial
pressure and the broadening gas pressures were similar (P_{CO_2} =
50 Torr, P_B = 80 to 700 Torr), however, the path length (6.35 cm)
and optical mass were smaller than that used here.

The data for the P(20) line of 10.4 μm (961 cm^{-1}) band by
Patty, et al., (1968) were originally published as broadening
coefficients for carbon dioxide with respect to the various gases.
These were converted to broadening factors with respect to nitrogen
by Eq. (2.4.6) which is

$$F_i = \frac{B_{N_2}}{B_i}$$

The data were obtained using a laser tuned to the P(20) line as a
source of radiation. The radiation passed through a multiple pass
cell and into a prism spectrometer set at the frequency of the P(20)
line. In these tests the cell length was approximately 4 or 8
meters. The carbon dioxide partial pressure was either 50 or 100
Torr, while the broadening gas pressure varied up to 250 Torr. The

TABLE VIII

BROADENING FACTORS FOR CARBON DIOXIDE

Band	Investigator	Type Measurement	Broadener					
			Argon		Helium		Oxygen	
			F	D_{ab}/D_{aN_2}	F	D_{ab}/D_{aN_2}	F	D_{ab}/D_{aN_2}
15 μm	This work	Band average	0.78	0.93	0.80	0.61	0.85	0.94
4.3μm (2350cm^{-1})	Burch et al., (1962a)	Band average	0.78	0.93	0.59	0.52	0.81	0.91
10.4μm P(20)(961cm^{-1})	Patty et al., (1968)	Laser	0.79	0.94	0.79	0.60	—	—
10.4μm P(20)(961cm^{-1})	McCubbin and Mooney (1968)	Laser	1.10	1.10	—	—	1.00	—
10.4μm P(20)(961cm^{-1})	Boutin et al., (1967)	Laser	0.70	0.88	0.85	0.63	0.81	0.92
4.3 μm	Coggeshall and Saier	Medium resolution	—	—	0.65	0.55	0.94	0.99
14.8 μm	Coggeshall and Saier	Single wavelength	—	—	0.78	0.60	0.98	1.02

experimental method was very similar to that used in Chapter 5 of this work for the determination of the broadening coefficient for carbon dioxide with respect to nitrogen. The short cell was filled with carbon dioxide to a pressure of approximately 100 Torr and the transmittance measured. The longer cell was then filled with the same optical mass of carbon dioxide (pressure approximately 50 Torr) and then the transmittance measured as a broadening gas was added. From a plot of transmittance versus broadening gas pressure, the broadening gas pressure at which the transmittance was equal to the transmittance of the pure carbon dioxide sample in the short cell could be determined. At equal transmittances it was assumed that the line half-widths were equal and the self-broadening coefficient was determined from Eq. (5.1.2)

$$ B = \frac{P_b}{P^S_{CO_2} - P^L_{CO_2}} $$

As was mentioned earlier, the self-broadening coefficients were divided into the self-broadening coefficient with respect to nitrogen, to derive the F values of Table VIII.

The results reported by McCubbin and Mooney (1968) were also determined using a laser as a radiation source. The experimental apparatus consisted of a carbon dioxide laser tuned to the P(20) line of the 10.4 μm (961 cm^{-1}) band, a multiple pass White cell, and a spectrometer set to the frequency of the line center. In this case, the spectrometer was a grating type instrument. The carbon dioxide partial pressure was 1 Torr and the broadening gas

pressure varied from zero to 30 Torr. The path length was 20.88 m. Broadening gases used were argon, air, and nitrogen. Transmittance was plotted as a function of gas pressure for the various broadening gases. Next, a family of theoreticl transmittance versus pressure curves was plotted for various line half widths using the Voigt profile line shape. The half width of the experimentally observed absorption line was then said to be equal to the half width of the theoretical line that produced the transmittance versus pressure curve best fitting the experimental data. The results were presented in the form of line half widths for the various broadening gases. These half widths (carbon dioxide self-broadened = 0.096, nitrogen broadened = 0.070, air broadened = 0.080, and argon broadened = 0.077) were converted to relative broadening factors by simple division of the foreign broadened half widths by the nitrogen half width.

In their work, Bouten et al., (1967) used a carbon dioxide laser tuned to the P(20) line of the 10.4 μm (961 cm^{-1}) band as a radiation source. A spectrophotometer, set to the wavelength of the line center, measured the radiation transmitted by a cell filled with carbon dioxide and a broadening gas. From the ratio of the absorption coefficients of a carbon dioxide sample and a foreign broadened sample they calculated the ratio of the squares of the collision diameters for carbon dioxide-carbon dioxide collisions and carbon dioxide-foreign gas collisions. The broadening factor presented in Table VIII were determined by first rewriting Eq. (2.4.4) in the form

$$B = \left(\frac{2M_b}{M_{CO_2} + M_b} \right)^{\frac{1}{2}} \left(\frac{D_{CO_2CO_2}}{D_{CO_2b}} \right)^2 \qquad (6.7.1)$$

and calculating the broadening coefficients for the various gases. These were then divided into the broadening coefficient for nitrogen (which had also been determined from the data of Boutin et al. by the above method) in accordance with Eq. (2.4.6). In their work Boutin et al. used carbon dioxide and broadening gas partial pressures that were high enough to ensure that collisional broadening determined the line profile.

Coggeshall and Saier (1947) determined the collision diameter ratios for carbon dioxide - carbon dioxide collisions and carbon dioxide - foreign gas collisions at a single wavelength in the 4.3 μm (2350 cm^{-1}) band and a single wavelength in the 15 μm (667 cm^{-1}) band. The method was similar to that used in Chapter 5 except that sample transmissivities were matched at a single wavelength rather than matching the integrals over the band. Test conditions and resolution resembled those used in these tests. The collision diameter ratios presented by Coggeshall and Saier were converted to broadening factors by means of Eq. (6.7.1) and Eq. (2.4.6).

It can be seen from the descriptions of the various techniques that the property being measured and the assumptions made in interpreting the data are quite different for the different techniques. For example, the technique using a black body radiation source (this work, Burch et al., (1962a) and Coggeshall and Saier (1947) is actually measuring a property of the wings of the lines (since

the sample required to achieve sufficient absorption to properly operate the spectrometer results in line centers being essentially opaque) while the techniques using a laser as a radiation source measure a property of a single line near the line center. With these differences in mind, the data presented in Table VIII can be compared.

In the case of argon, all of the measurements except that of McCubbin and Mooney are in relatively close agreement, the differences probably being within the experimental errors. (Boutin et al., (1967) considered their value to be in good agreement with that of Burch et al., (1962a)). The measurement by McCubbin and Mooney (1968) is significantly different from the other (1.10 as compared to 0.78). The difference between his results and those of Burch were noted by McCubbin in his paper, but no explanation was offered. It should be noted that this work, the work of Burch, et al., (1962a) and the work of Patty, et al., (1968) were all performed at pressures considerably higher than the work of McCubbin and Mooney. It is quite possible that the difference is in some way attributable to this. Another possibility is that the measurements of Patty, et al., (1968) may not have been made at precisely the same frequency as those of McCubbin and Mooney. McCubbin and Mooney used a carbon dioxide-nitrogen laser because, as they said, an increased pressure of a carbon dioxide-nitrogen-helium laser (as used by Patty et al., (1968)) might permit oscillation away from the exact center. Although Patty, et al., (1968) used a carbon dioxide-nitrogen-helium laser, this author is not able to judge as

to whether or not the pressure was high enough to allow this shift in frequency to occur. Resolution of this difference will have to be made by those who are more knowledgeable in the area of laser operation.

In the case of helium broadening, it is seen that this work and the works of Boutin et al., (1967), Patty et al., (1968),and Coggeshall and Saier (1947) at 14.8 μm are in good agreement. These differ significantly from the values obtained by Burch et al., (1962a) for the 4.3 μm band and Coggeshall and Saier (1947) at 4.3 μm. It appears that the effects of a given broadener may differ for different absorption bands of an absorber, however, one would not expect the differences to be too great. The test conditions for our work and the work of Burch et al. and the work of Coggeshall and Saier (particularly in the case of the 8.74 cm sample) are not greatly different so that the relative contributions of line centers and line wings should not be too different. A check on the accuracy of our work will be obtained when the wavelength dependence of the self-broadening coefficient of carbon dioxide with respect to the various gases in discussed in the next chapter.

The data for oxygen also pose a problem. Although our data, the data of Burch et al., (1962a), the data of Boutin et al., (1967) and the data of Coggeshall and Saier (1947) agree fairly well there is a rather significant difference with the work of McCubbin and Mooney who used air as a broadener. They measured a broadening factor of 1.14 for air broadened carbon dioxide. Since air is composed principally of nitrogen and oxygen, this result could be

taken to mean that oxygen is a more effective broadener than nitrogen. This is in direct disagreement to our results and the results of the other researchers cited here.

One other point that might be noted is the similarity of the broadening factors for helium and argon. Patty has noted that this should not be entirely unexpected because, although helium will collide more frequently with carbon dioxide (and hence should cause a larger half width, according to the simple theory used here) its polarizability is lower and should have a smaller effect. A qualitative check on the equality of the broadening coefficients for these two gases will be examined in the next chapter when the wavelength-dependent broadening coefficients are discussed.

It is apparent from the foregoing discussion that explanations for the similarities and differences between the broadening effects of the gases studied and between the work of various investigators are not available. Hopefully, further theoretical and experimental work will produce a consistent picture.

CHAPTER 7

WAVELENGTH DEPENDENT BROADENING COEFFICIENTS

7.1 Introduction

Although the band-averaged self-broadening coefficient and

relative broadening factors discussed in Chapters 5 and 6 give

some indication of the effects of various broadening gases on the

absorption of infrared radiation by carbon dioxide, they still leave

an incomplete picture. In view of this a study was undertaken of

the wavelength dependence in the 15 μm band of the broadening coef-

ficients. The coefficients were measured in the region from

588 to 741cm^{-1}(17 to 13.5 μm) using argon, helium, nitrogen, and

oxygen as broadening gases. Most of the measurements were taken

at a single carbon dioxide partial pressure, although limited data

were obtained from 635 to 700cm^{-1}(15.75 to 14.25 μm) at a second

partial pressure. Cell lengths were varied depending upon the

region of the band being investigated.

The wavelength dependence of the broadening coefficient of

carbon dioxide with respect to nitrogen has previously been investi-

gated by Burch, et al., (1962), in the 15 μm (667 cm^{-1}) region, by

Anderson et al., (1967) in the 4.3 μm(2,350 cm^{-1}) region, and by

Vasilevskii et al., (1967) in the 2.06 μm (4,854 cm^{-1}) region.

The techniques have varied, the work of Burch et al., (1962) and

Anderson et al., (1967) having been performed at medium resolution

while the work of Vasilevskii et al., (1967) was performed at high

resolution. As far as is known, the wavelength dependence of the

broadening coefficient with respect to other broadening gases has
not been investigated in the 15 μm region.

7.2 Experimental Method

The data were obtained using the Model 221 Spectrophotometer,
the Perkin Elmer long path cells, the 8.74 cm and 2.02cm short
cells, and the Baratron pressure gauge. The data were read from
the instrument strip chart recorder.

The experimental technique was similar to that used by Burch,
et al., (1962). This technique is a variation of that used for
determining the band-averaged broadening coefficients. Here a
short cell is placed in the reference beam of the instrument and
a longer cell in the sample beam. Equal optical masses of carbon
dioxide are then placed in the two cells. Due to the decreased
pressure in the long cell, the absorption in it (the sample beam)
is less than the absorption in the short cell (the reference beam).
As a broadening gas is added to the long cell, the absorption
increases (although not uniformly at all wavelengths). When the
absorption in the long cell, at any wavelength, equals the absorption
in the short cell at that wavelength, one can calculate the broad-
ening coefficient by means of an equation similar to Eq. (5.1.2).

$$B = \frac{P_B}{P_{CO_2}^S - P_{CO_2}^L} \qquad (7.1.1)$$

It is desirable that the sample in the reference beam be chosen
so that its transmissivity is between 10 and 90 percent; this gives

most satisfactory instrument accuracy. If the transmissivity is less than 10 percent, the signal levels driving the nulling servo become very small and noise and scattered radiation become important. If the transmissivity is greater than 90 percent, the effects of changing broadening gas pressure become small.

In this work, two sets of cells were used, depending upon the wavelength interval being investigated. A 2.02cm reference cell paired with an 8.74 cm sample cell was used during studies of the region from 641 to 695cm^{-1}(15.6 to 14.4 μm), while a 400 cm reference cell paired with a 1,600 cm sample cell was used while studying the regions from 719 to 763cm^{-1}(13.9 to 13.1 μm) and 581 to 621cm^{-1} (17.2 to 161 μm). Unfortunately, we were unable to obtain over-lapping wavelength intervals; this would have required a set of cells of intermediate length.

The optical path was purged with dry nitrogen, as usual, and adequate time was allowed to insure sample gas mixing in the cells (aided by a fan in the case of the long path cells). All measurements for a particular broadening gas in a particular wavelength interval were performed in a single session.

7.3 Data Processing

It was anticipated that the data reduction would follow the method outlined by Burch, et al., (1962). In that method, the wavelength interval under study is scanned with the cells evacuated. This defines the line of equal beam transmissivities. The samples are then placed in the cells and spectra scanned at different broadening gas pressures. One can then determine the wavelength

of the intersections of the various curves with the line of equal transmissivity, determine the value of the broadening coefficient at each intersection, and plot the value of the broadening coefficient as a function of wavelength or wavenumber.

Several difficulties were encountered in attempting to use this technique. First, it was found that the ratio of the transmissivities of the two beams was very nearly equal to one (generally the variation would be less than 5 percent) for any given broadening gas pressure. This caused the traces to cross the equal transmissivity line at a small angle, making it very difficult to locate the intersection point accurately. This difficulty was somewhat alleviated by expanding the transmissivity scale by a factor of ten and the wavelength scale by a factor of two. When this large scale factor expansion was used, however, it became obvious that the small non-repeatability in the instrument scale factor (mentioned in section 4.3) combined with the small intersection angle of the traces was causing a large amount of data scatter. This scatter had been present previously, but it became much more noticeable in the expanded scale situation. It also became apparent at this time that the broadening coefficient versus wavelength plot would contain more fine structure than had been anticipated. To define this structure, it appeared that very closely spaced broadening gas pressures would be required. However, the noise on the signal set a finite lower limit on broadening gas pressure increment. After several attempts to use this method had failed, it was concluded that it was not a practical method for use with our equipment.

It seemed that there was a basic difficulty, inherent in the method, that placed severe limitations on it, viz, that the method made use of a very small part (less than 1 percent) of the available information. Only the intersection point of two lines was used; the remainder of the information was ignored.

In an effort to overcome some of the difficulties outlined above, a data reduction scheme was developed to use as much of the available information as possible. This technique was used to determine the broadening coefficient in all cases except for part of the helium data. Because of the unusual nature of the data for helium it was possible to use the method described by Burch, et al. The method used for a particular section of data is indicated on the helium plot. The method used for the reduction of the remainder of the data consisted of the following steps:

1. The wavelength region under examination was scanned three or more times with the cells evacuated. The traces were superimposed. A typical result is shown in Figure 10.

2. The cells were filled with carbon dioxide at the proper pressures.

3. The wavelength region was scanned for several roughly-evenly spaced broadening gas pressures. Generally, five to seven broadening gas pressures were used. A typical example of the instrument strip chart record is shown in Figure 11; the particular record shown is for argon.

4. A tracing of the three equal transmissivity lines and of the smoothed sample traces was made. Wavelength and transmissivity
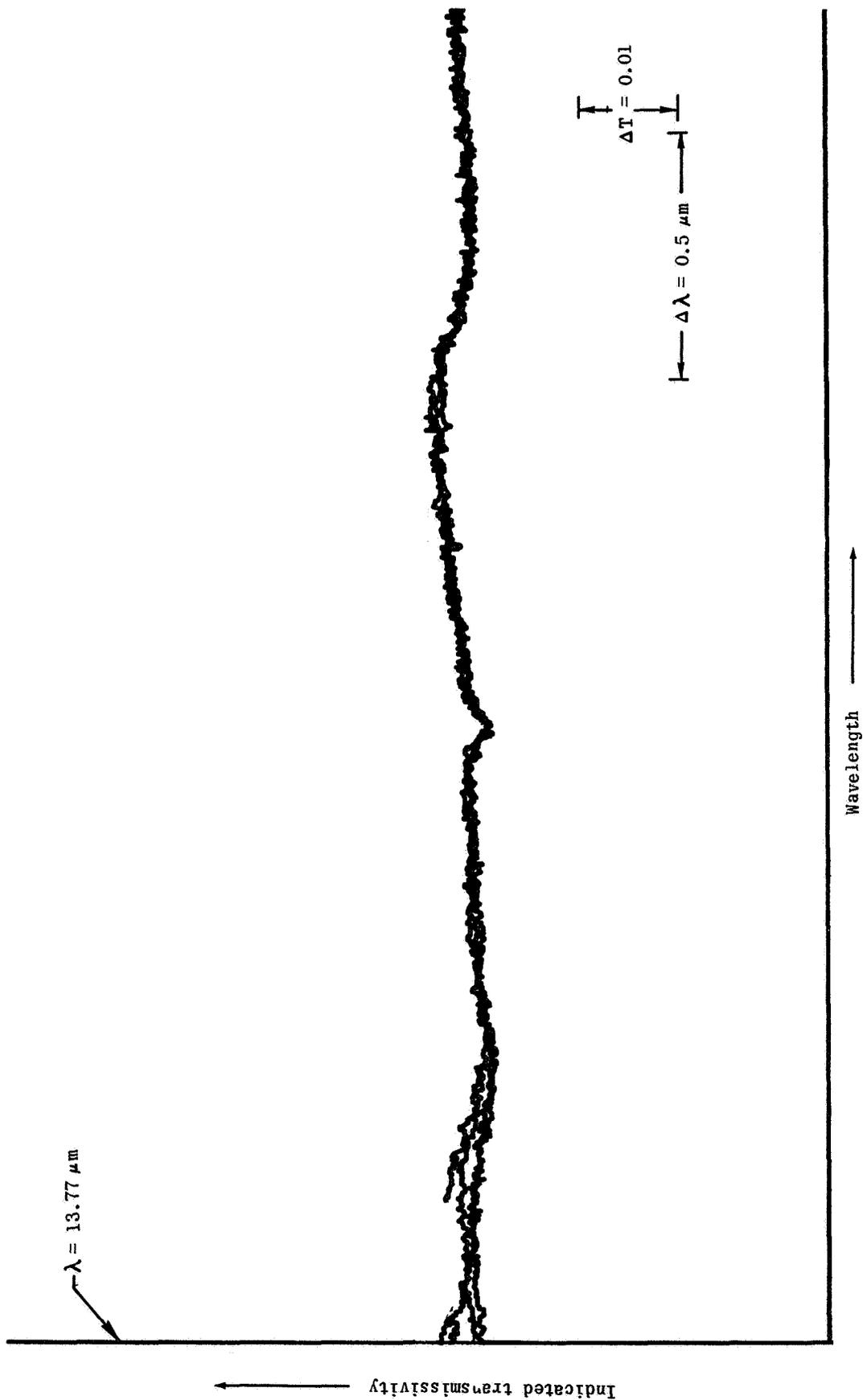
Figure 10.- Line of equal sample transmissivities, 2.02 cm reference cell, 8.74 cm sample cell.

$\lambda = 13.77 \ \mu m$

Ref
$P_{CO_2} = 400$

Sam
$P_{CO_2} = 92.66$

Sam
$P_A = 515.2$
530.
545.
560.
574.45

$\Delta T = 0.01$

$\Delta \lambda = 0.5 \ \mu m$

Indicated transmissivity

Wavelength
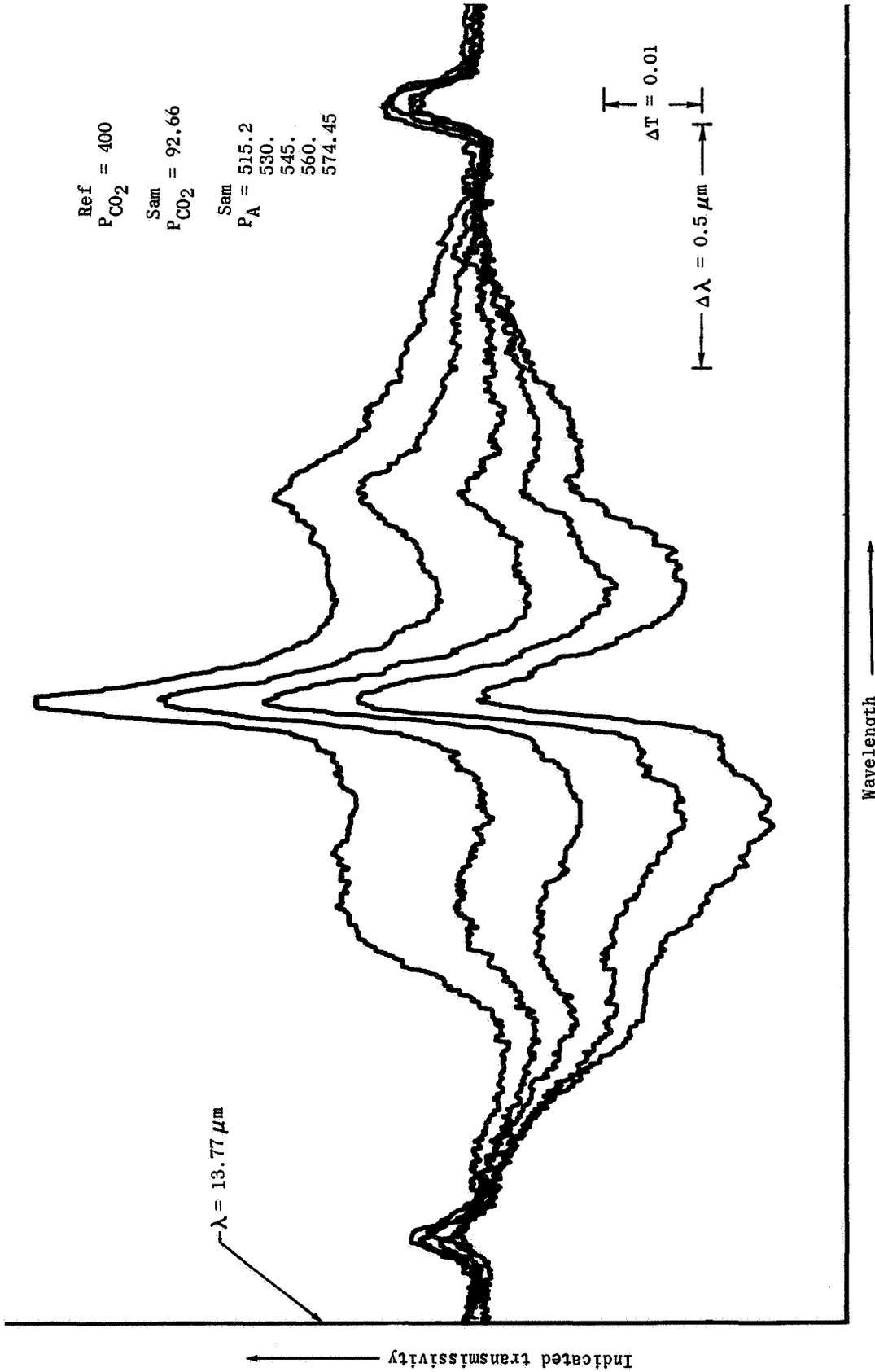
Figure 11.- Instrument output for argon broadened carbon dioxide sample.

scales for the two plots were aligned using reference marks placed on the paper at the time the data were run. The tracing of the equal transmissivity lines of Figure 10 and the argon data of Figure 11 is shown in Figure 12.

5. Cross plots of transmissivity ratio versus

$$\frac{P_B}{P_{CO_2}^S - P_{CO_2}^L}$$

at constant wavelengths were made. Typical examples (again for the argon data) are shown in Figure 13.

6. The value of the broadening coefficient could then be read from the cross plot at the intersection of the faired curve with the line indicating a transmissivity ratio equal to one.

7. The broadening coefficient was plotted as a function of wavenumber. When these curves were faired, the pattern of the instrument strip chart record (of which Figure 11 is an example) was examined to determine if the structure appearing on the $B(\nu)$ plot consisted of variations in the data or only noise.

7.4 Results

Plots of carbon dioxide broadening coefficients with respect to the various broadening gases are shown in Figures 14, 15, 16, and 17. These were determined at the test conditions indicated on the various figures. The symbols indicate the points at which the broadening coefficient was determined. The determinations were made using the cross plotting technique described in section 7.3, except

88
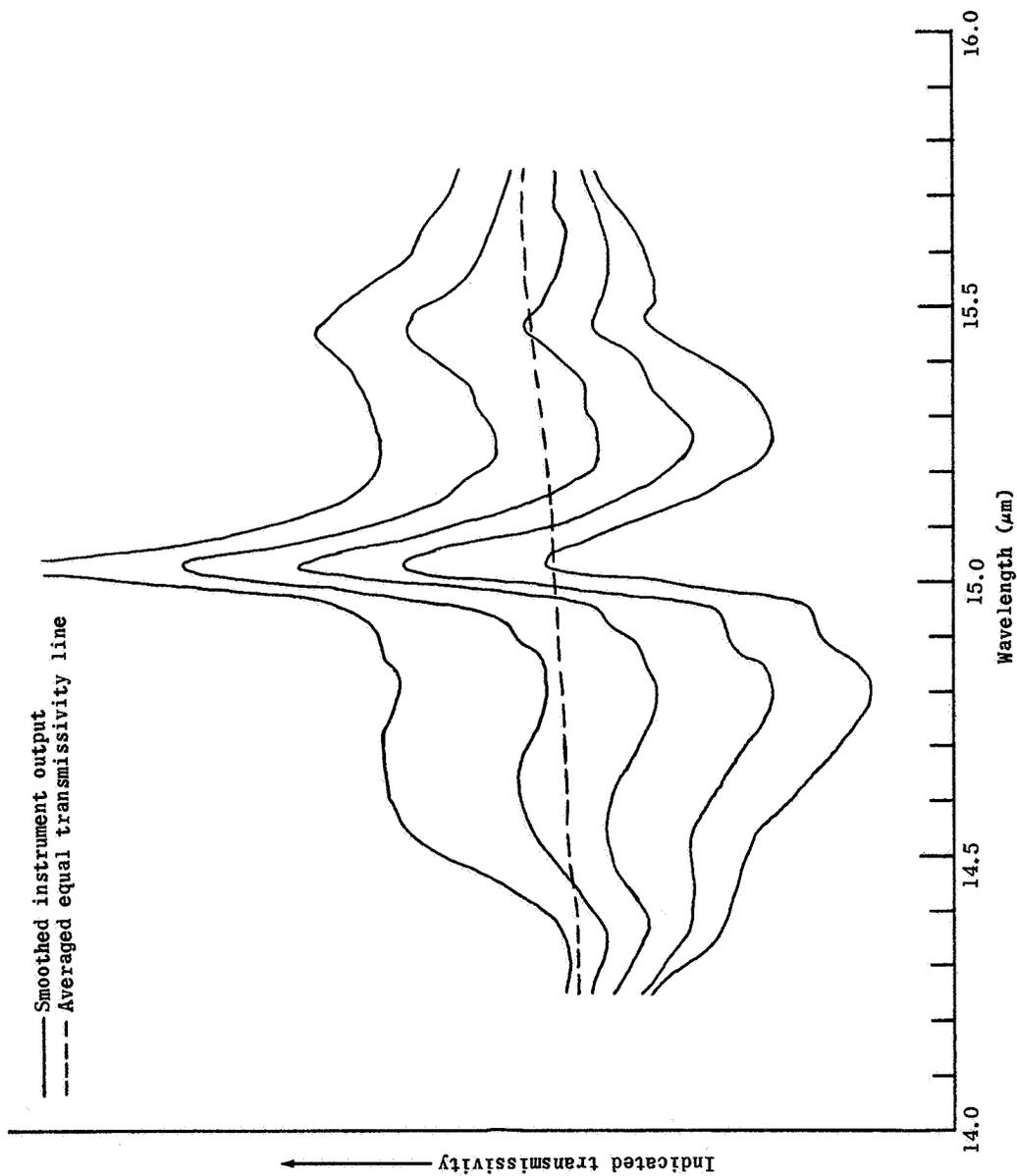
Figure 12.- Smoothed instrument output and averaged line of equal sample transmissivities for argon broadened carbon dioxide.
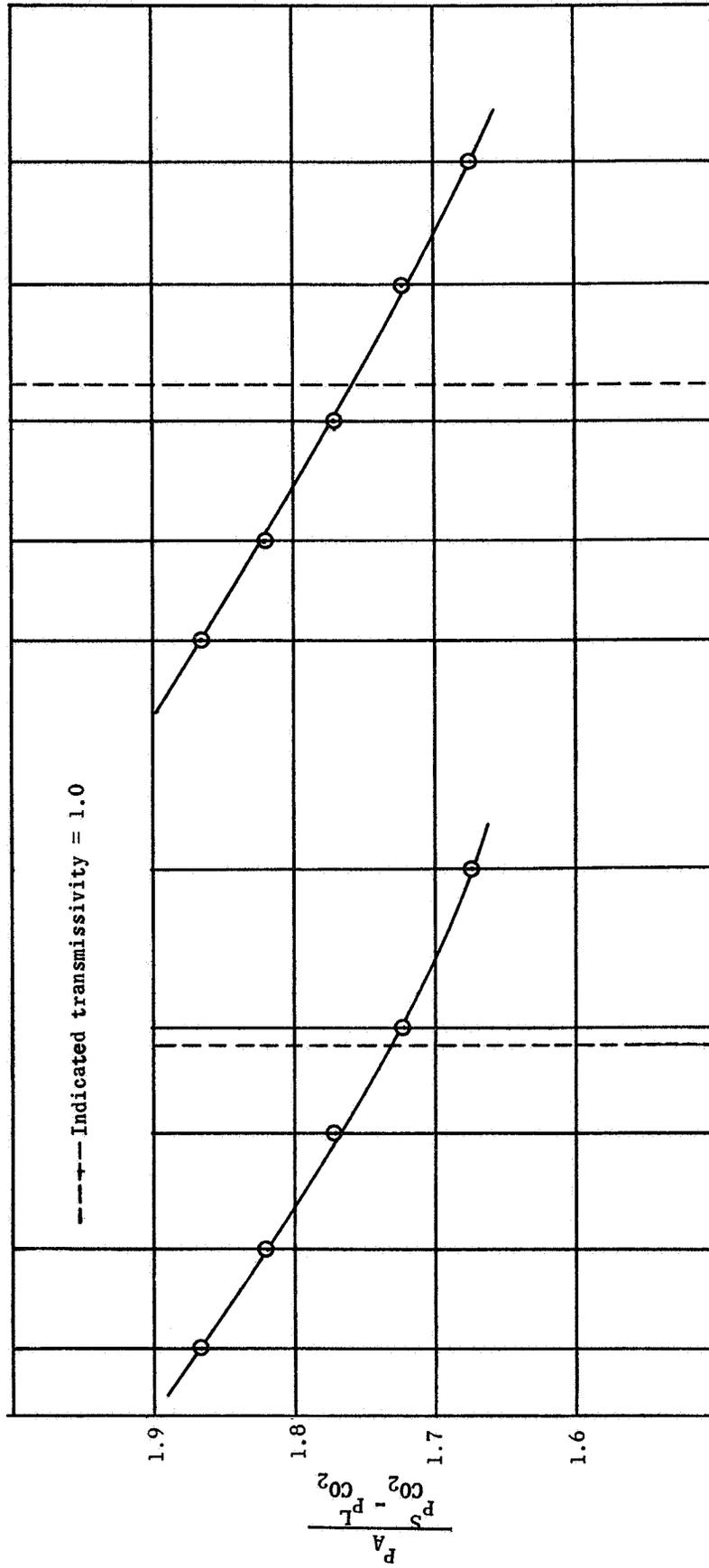
(a) $\nu = 673.4$ cm^{-1}.

(b) $\nu = 668.9$ cm^{-1}.

Figure 13.— Crossplots of instrument output for $B(\nu)$ determination.

Figure 13.- Concluded.
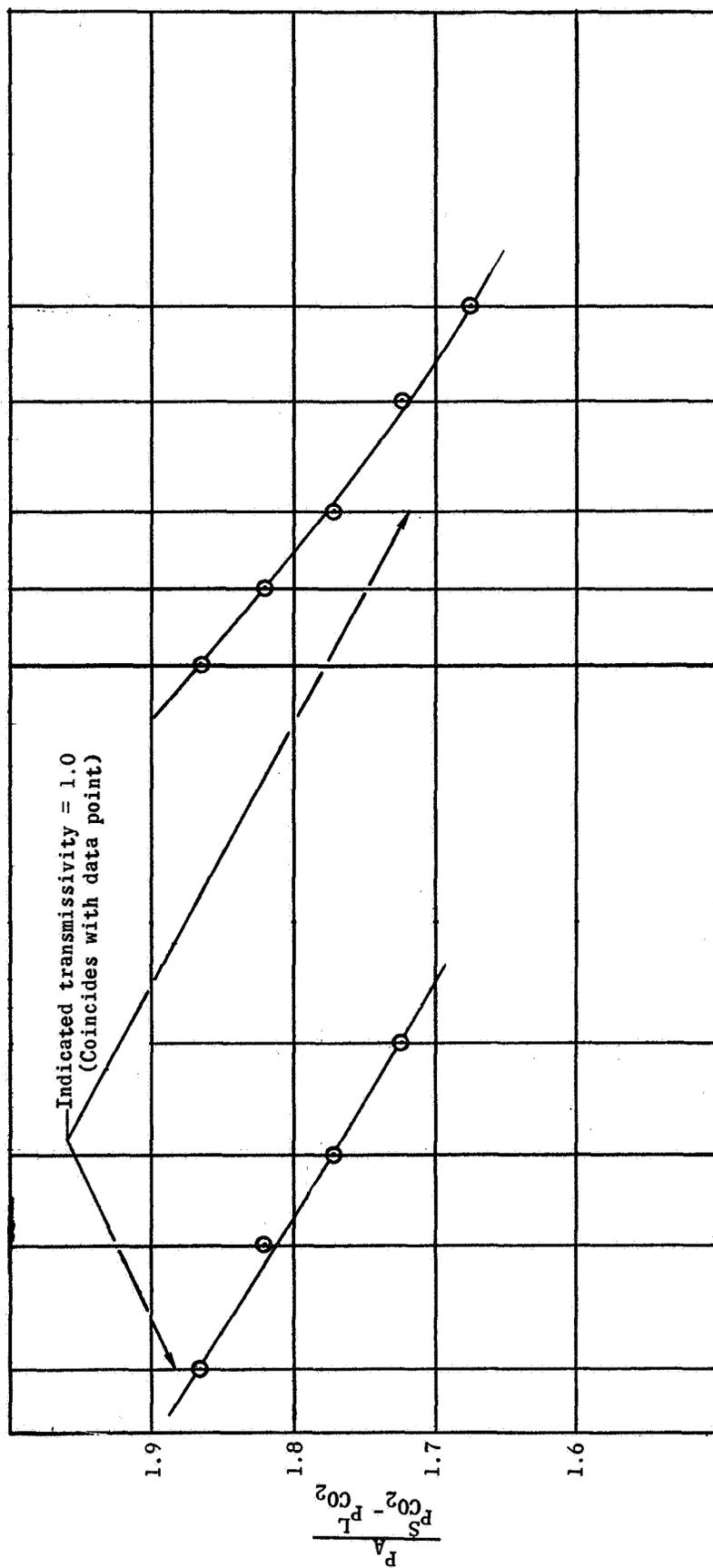
(c) $\nu = 664.5$ cm^{-1}.

(d) $\nu = 660.0$ cm^{-1}.
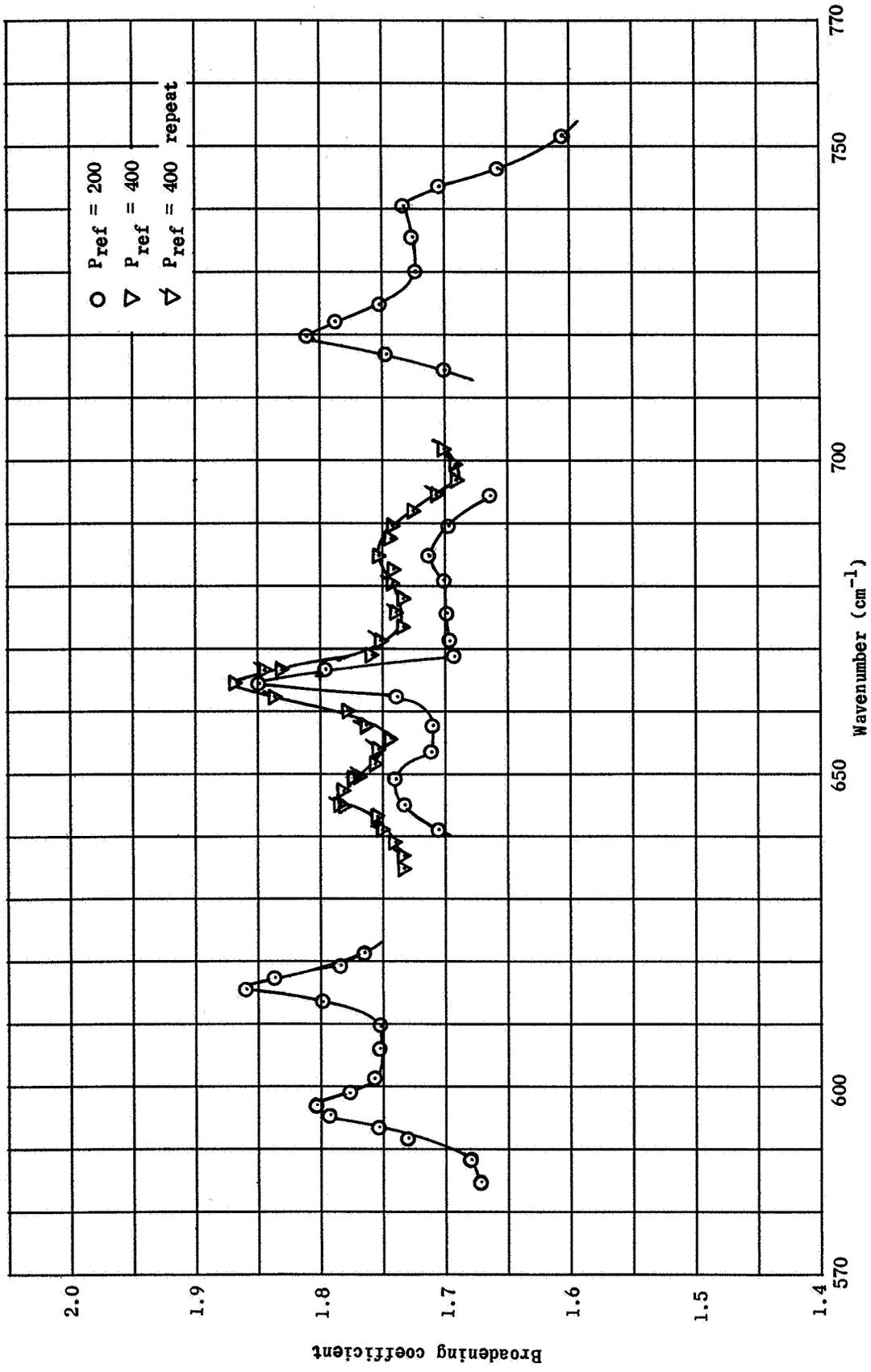
Figure 14.- Broadening coefficient for argon vs. wavenumber.
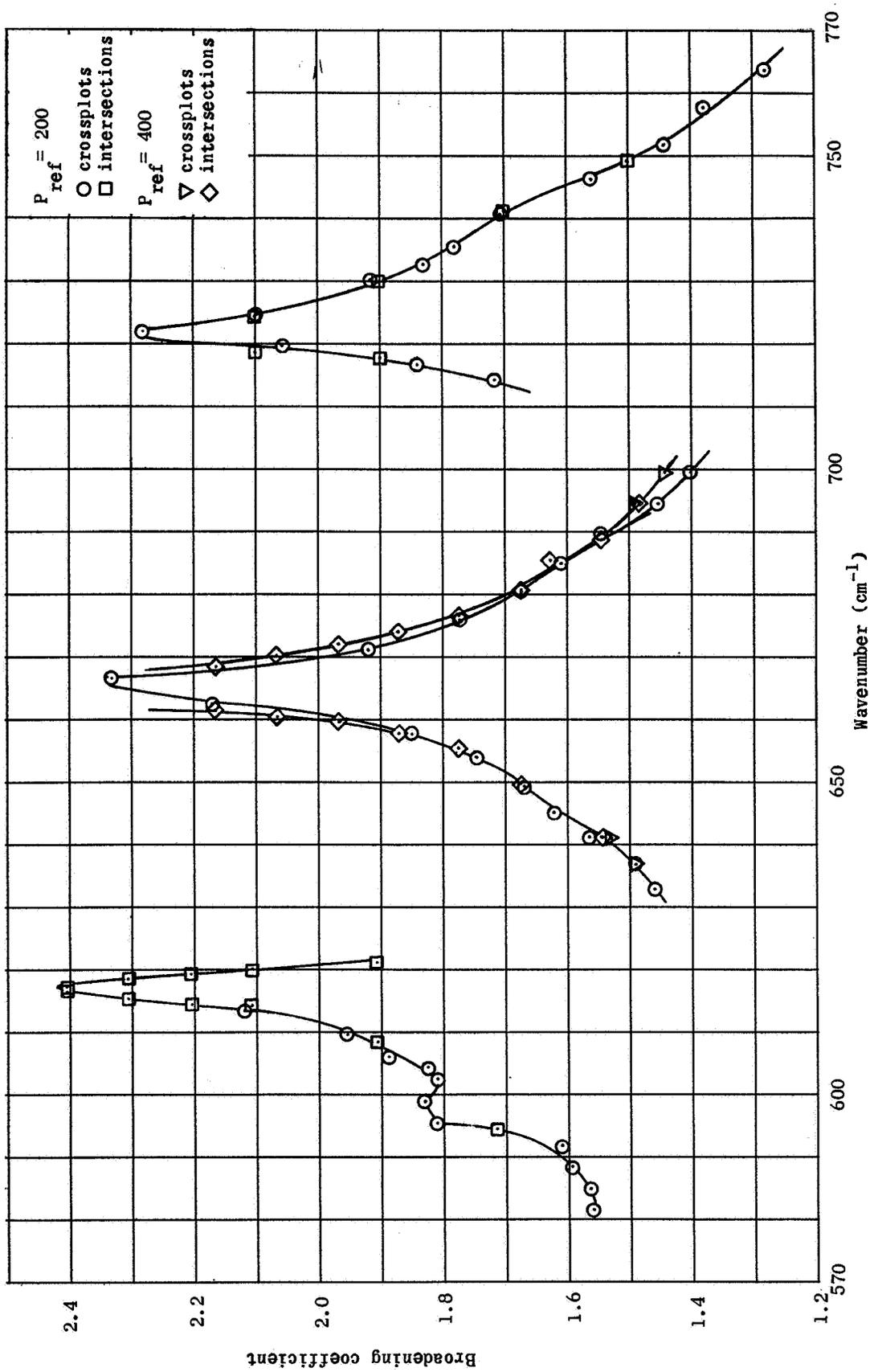
Figure 15.- Broadening coefficient for helium vs. wavenumber.
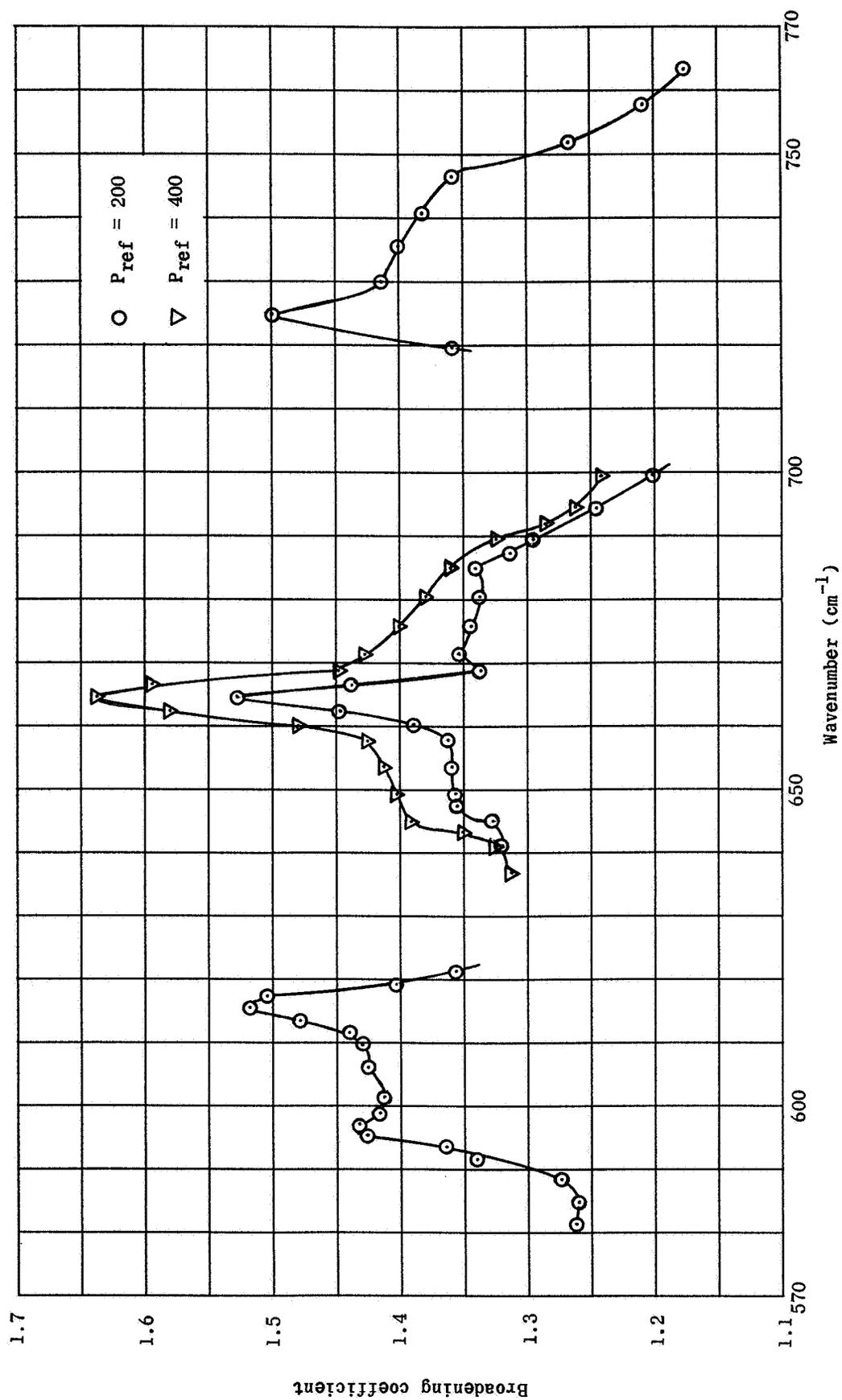
Figure 16.- Broadening coefficient for nitrogen vs. wavenumber.
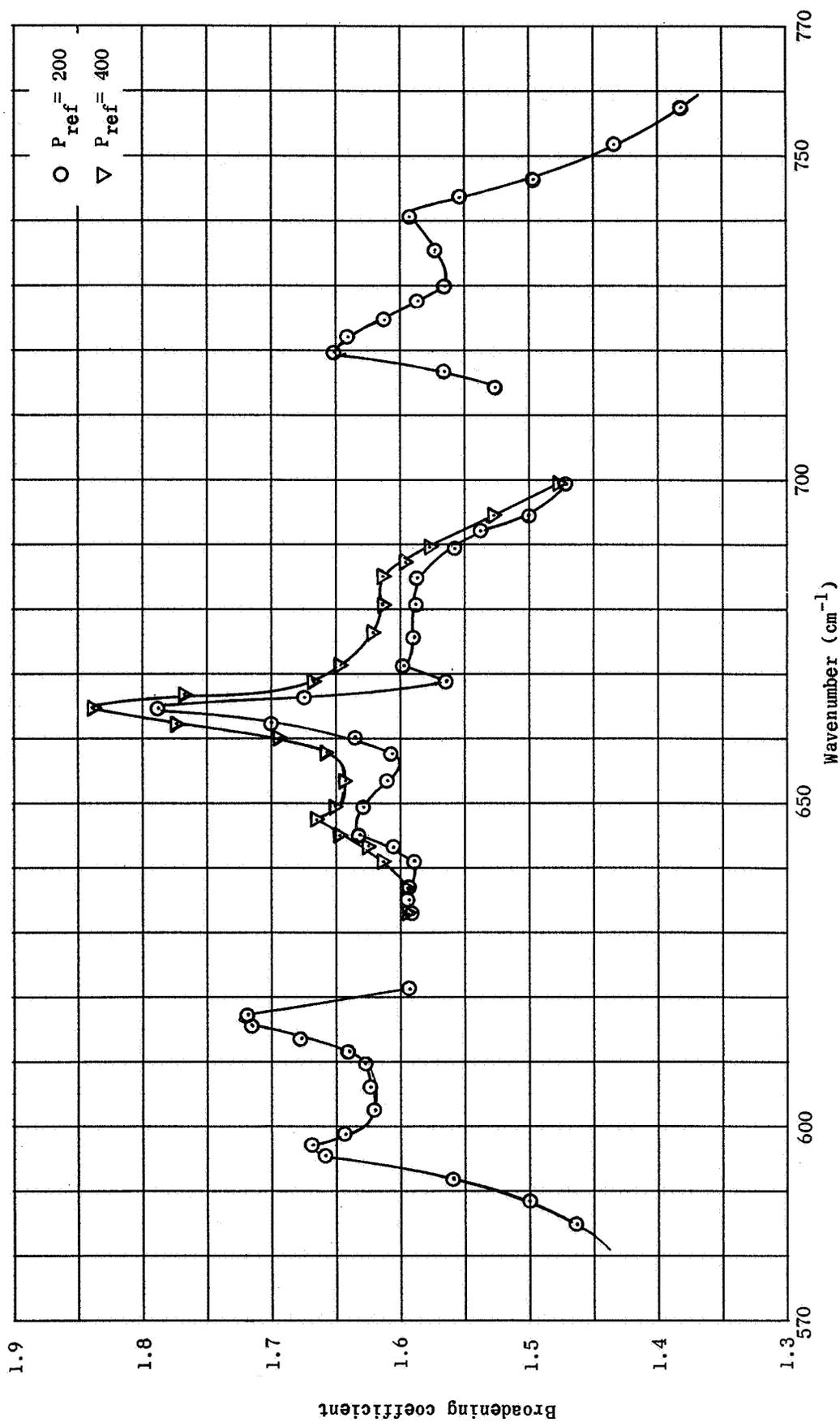
Figure 17.- Broadening coefficient for oxygen vs. wavenumber.

except in the case of helium where many of the points were deter-
mined using the intersections of the traces with the line of equal
sample transmissivity. It was feasible to reduce the helium data
in this way because the intersections of the traces and the equal
transmissivity line were steep. It should be noted that the broad-
ening coefficient scale on the plots for helium has a different
scale factor than that of the other plots.

7.5 Accuracy

Although this technique is subject to the same basic difficulty
of matching optical masses as is the technique for measuring the
band-averaged broadening coefficient of Chapter 5, we might expect
the final result to be somewhat more accurate. This is because
the measurements of samples of different lengths are made at the
same time (reducing the problem of instrument drifts) and because
a large part of the data processing system is eliminated. Uncer-
tainties in optical masses, pressures, instrument drifts, gas com-
position, and data reduction errors still exist. A measure of the
repeatability of the system can be obtained from the data for argon
in Figure 14. The plot shows two sets of data taken four days apart.
It can be seen that the data are slightly shifted, but obviously
the repeatability is very good. Based on these considerations a
reasonable value for the 1σ error in the value of the broadening
coefficient is 0.05.

A major error would probably take the form of a shift in the
curve of self-broadening coefficient versus wavelength rather than
producing a radical change in shape of the curve. This conclusion

is based on the fact that improperly formed samples (small errors in carbon dioxide partial pressure, generally) tended to produce results of the same general shape, but of shifted value. The shape was modified somewhat, but the main features were essentially unchanged.

7.6   Discussion

7.6.1   Introduction

The results of the investigation of the wavelength dependence of the carbon dioxide broadening coefficient with respect to argon, helium nitrogen, and oxygen are presented in Figures 14, 15, 16, and 17. It will be noted from the figures that the broadening coefficient is variable with wavelength, and that the shape of the curves is similar for argon, nitrogen and oxygen, but that helium behaves differently from the other gases. In this section these results will be compared with the previous determinations of the band-averaged broadening coefficients and with the work of others wherever possible. The shape of the curves will be discussed and some possible explanations offered.

7.6.2   Comparison with the Band Averaged Broadening Factors

In the discussion of the band averaged broadening factors of Chapter 6, it was noted that argon and helium were of approximately equal effectiveness (on the average) for broadening carbon dioxide absorption lines in the 15 μm region. The band averaged broadening factors were determined to be 0.80 for helium, 0.78 for argon and 0.85 for oxygen. This result differed from that obtained by Burch et al., (1962a) in the 4.3 μm (2350cm^{-1}) band where the broadening

factors were found to be 0.59 for helium, 0.78 for argon, and 0.81 for oxygen.

To make a really valid comparison between the band averaged data of Chapter 6 and the wavelength dependent data, it would be necessary to determine a weighted average of the wavelength dependent data. The weighting function, which would be different for each gas, would be determined by the absorption at each wavelength. Rather than undertaking this task, the arithmetic mean of the data for each gas was found. This is equivalent to saying that the weighting function is equal to one. So long as we are taking ratios between the gases and the character of the absorption is not greatly different for the various gases the results should be reasonably accurate. Table IX displays the means of the wavelength dependent broadening coefficients for the wavelength region from 645 to 690 cm^{-1} (15.5 to 14.5 μm) and a carbon dioxide partial pressure in the reference cell of 200 Torr. (This is the condition most closely approximating the conditions under which the band averaged factors were determined). Also shown in Table IX are the "broadening factors" computed from these means and the broadening coefficient and relative broadening factors from chapters 5 & 6.

It can be seen that the mean of the broadening coefficient with respect to nitrogen and the broadening factors determined by dividing the means of the broadening coefficients with respect to the other gases into the mean of the broadening coefficient with respect to nitrogen agree quite well with the previously determined band averaged broadening data.

TABLE IX

COMPARISON OF MEANS OF WAVELENGTH DEPENDENT COEFFICIENTS

WITH BAND AVERAGED BROADENING FACTORS

Gas	Band Averaged Data		Mean of Wavelength Dependent Data	
	B	F	B'	F'
N_2	1.30		1.37	
O_2		0.85	1.62	0.85
A		0.78	1.72	0.80
He		0.80	1.76	0.77

As was found previously, argon and helium have approximately

equal broadening factors (although the order is interchanged - not

surprising in view of the differences in the shape of their curves

of broadening coefficient versus wavenumber), The broadening

factor for oxygen is again somewhat higher. Although one must be

careful not to attach too much significance to these mean values,

it is safe to say that these results support the previous data in

that the band averaged broadening factors for argon and helium

are very nearly equal in the 15 μm region as had been found in the

work discussed in chapter 6.

7.6.3. Structure of the wavenumber dependent broadening coefficients

Before comparing the data obtained in this study with the work

of others, it is reasonable to look for an explanation for the peaks

in the plots of broadening coefficient versus wavelength. The

graphs show that the peaks consistently appear in the results

obtained for the various gases. The peaks are most pronounced for

argon, nitrogen, and oxygen while for helium fewer peaks are evident.

As a first step the wavenumber at which the peaks appear and

their relative heights were read from the plots; these are shown in

Table X for argon, nitrogen and oxygen. Because of its unusual

behavior helium was not considered in this analysis. Table XI

(Drayson et al., 1968) displays the positions and strengths of the

major carbon dioxide bands that occur in the wavenumber region where

the broadening coefficient has been measured. A comparison of

Table X with Table XI shows that there is close agreement between

the positions of the centers of the absorption bands and the positions

TABLE X

POSITIONS AND RELATIVE HEIGHTS

OF BROADENING COEFFICIENT MAXIMA

ν (cm^{-1})	λ (μm)	Relative Peak Height O_2	A	N_2
741	13.5	6	6	5
722	13.85	4	3	3
687	14.55	7	7	7
667	15.	1	1	1
645	15.5	5	5	6
617	16.2	2	2	2
595	16.8	3	4	4

TABLE XI

BAND INTENSITIES

BAND Center ($^{12}C^{16}O_2$)	INTENSITY $(cm^{-1} (atm\ cm)^{-1}_{300^{\circ}K}$ at $300^{\circ}K$)
667.379	$194^{(1)}$
618.033	$4.27^{(1)}$
720.808	$5.04^{(4)}$
667.750	$15^{(4)}$
647.054	$1.0^{(1)}$
791.447	$0.022^{(2)}$
597.337	$0.14^{(1)}$
741.730	$0.12^{(4)}$
668.151	$0.85^{(2)}$
688.672	$0.3^{(3)}$
544.279	$0.004^{(1)}$
581.62	$0.0042^{(2)}$
757.47	$0.0059^{(2)}$
828.284	$0.00049^{(2)}$
738.364	$0.014^{(2)}$

(1) Madden (1961)

(2) Yamamoto and Sasamori (1958)

(3) Yamamoto and Sasamori (1964)

(4) Drayson et al., (1968)

of the maxima of the curves of broadening coefficient. Considering

those bands having centers located within a few cm^{-1} of each other

to be single bands and rank ordering the bands in terms of their

strengths (This lumping of adjacent band is felt to be justified

since the instrument resolution is approximately 5 to 6 cm^{-1} in

these tests) produces the results shown in Table XII.

TABLE XII

RANK ORDERING OF ABSORPTION BANDS BY BAND STRENGTH

(cm^{-1})	Band Intensity $(cm^{-1} (atm\ cm)^{-1}$ at 300K)	Rank
667 (667.379+667.750+668.151)	210.	1
720.81	5.0	2
618	4.27	3
647.1	1.00	4
688.7	0.30	5
597.3	0.14	6
741 (741.7+738.4)	0.13	7

A scatter diagram of the rank order of the height of a peak in the

plot of the wave number dependent broadening coefficient at a given

frequency versus rank order of the band strength at that frequency

was plotted, and is shown in Figure 18. This plot shows that the

height of the peak of the broadening coefficient tends to be cor-

related with the strength of the absorption band at the same frequency.

The correlation is not perfect, since this rather crude analysis does
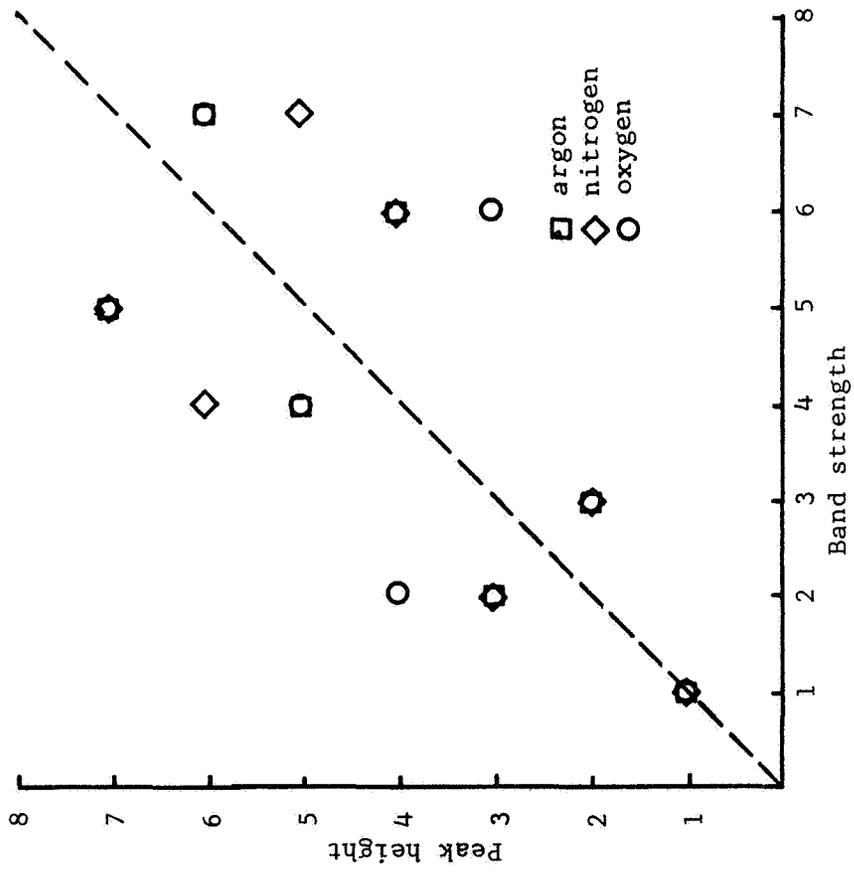
Figure 18. Scatter plot of peak height versus band strength

not consider such factors as data error, proximity of other bands,
or the validity of the measure of the peak importance (possibly
peak area is more relevant than peak height).

7.6.4 Comparison with other experimental work

For the 4.3 μm (2350cm^{-1}) band, Anderson et al., (1967) found that
the broadening coefficient with respect to nitrogen varied smoothly
from 1.2 to approximately 1.5. In general, the broadening factor
increased with increasing absorption, but the sharp peaking found
in the 15 μm band was not evident. The measurements were made at
a resolution similar to that used in this research. Vasilevskii
et al., (1967), found that the broadening factor for the 2.06 μm
(4850 cm^{-1}) band using nitrogen as a broadening gas varied from
1.5 to 2.13. Their measurements were made at high resolution, and
the data were obtained by nitrogen-carbon dioxide mixture. The
variation of broadening coefficient across the band was smooth.

There are two main differences between the near infrared
bands investigated in the above studies and absorption bands in
the region. First, the 4.3 μm(2350cm^{-1}) and 2.06 μm(4855cm^{-1})

bands are single absorption bands, while the
15 μm(667cm^{-1}) band consists of several overlapping bands. Second,
the 4.3 μm(2350cm^{-1} band and the 2.06 μm(4855cm^{-1}) band are parallel
bands while the bands in the 15 μm(667cm^{-1}) region are perpendicular
bands. Either one of these factors could influence the data
obtained in this investigation.

Figure 19 displays plots of the broadening coefficient with
respect to nitrogen in the 15 μm region at reference cell pressures
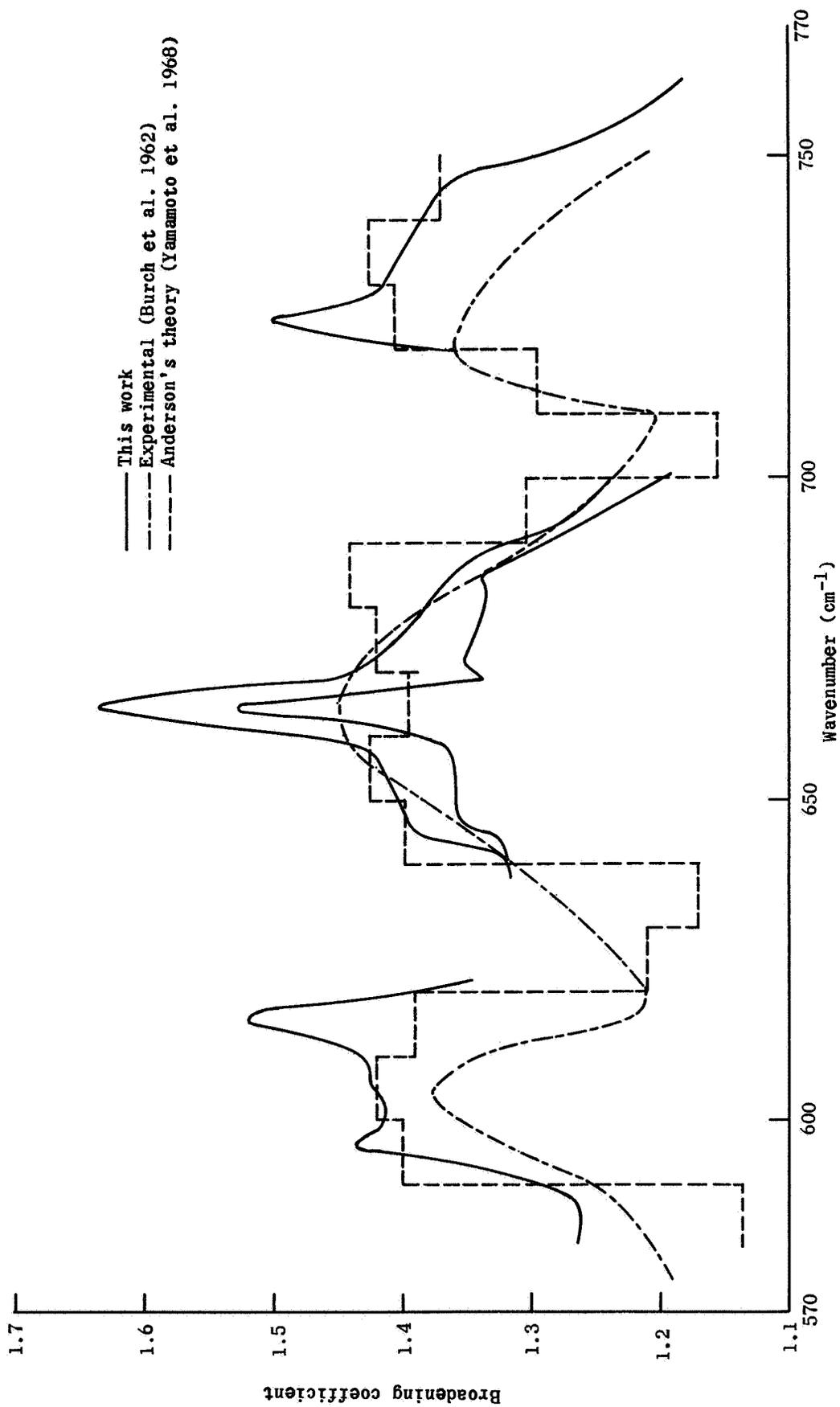
Figure 19.- Comparison of experimental and theoretical wavenumber dependent broadening coefficients for nitrogen.

of 400 Torr and 200 Torr. Also shown, for comparison, are the results obtained by Burch et al., (1962). The test conditions used by Burch et al., (1962) are unknown except that total pressures were restricted to less than one atmosphere. Because of the general similarity of their instrumentation to that used here, the test conditions were probably similar.

The curves shown in Figure 19 are generally similar in shape and mean value, but the data of Burch et al., (1962) are considerably smoother. This could be due to the Model 221 spectrophotometer which was used in making the measurements presented in this discussion being equipped with a brighter source than their Model 21 spectrophotometer. This allowed a somewhat higher resolution to be used than was available to them. Although lower resolutions was not used in an attempt to match their data, it is known from some very limited tests that the height of the sharp peak at 15 μm (667cm^{-1}) tends to increase with increasing resolution.

In the regions from 588. to 625cm^{-1} (17 to 16 μm) and from 714 to 770cm^{-1} (14 to 13 μm) the differences between the two sets of measurements cannot easily be accounted for simply by differences in instrument resolution (as the differences in the region from 645 to 690cm^{-1} (15.5 to 19.5 μm) might be. If some shifting and smoothing is allowed the data could be placed in reasonably good agreement.

In view of the differences in test apparatus and our lack of information concerning the test conditions under which the data of Burch et al., (1962) were taken, the agreement between the two sets

of data is probably reasonably good.

7.6.5. Comparison with Theory

If all the lines of an absorption band had equal half width
and Lorentzian shape, the value of the broadening coefficient would
be constant with wavelength and equal to the ratio of the half width
of the self-broadened lines to the half width of the foreign gas
broadened lines. Madden (1961) showed that the half widths of
carbon dioxide absorption lines in the 15 μm region vary with
rotational quantum number. It also appears that the variation
depends on the broadening gas used; this was indicated in the
measurements made by Vasilevakii et al., (1967) for the 2.06 μm
(4855cm^{-1}) band and is probably true in the 15 μm (667cm^{-1}) region.
These effects would cause the value of the broadening coefficient
to vary with wavelength and broadening gas. Because of the com-
plexity of the absorption band in the 15 μm (667cm^{-1}) region and
the lack of information on the variation of line width with rotational
quantum number and broadening gas composition in the 15 μm(667cm^{-1})
region, it is not possible to predict the shape of the broadening
coefficient variation with wavelength in terms of the simplified
theory discussed in Chapter 2 of this report.

An example of a more sophisticated theoretical approach is
the theory developed by Anderson (1949) which was discussed in
Chapter 2. Anderson's line broadening theory as refined by Tsao and
Curnutte (1962) has been applied to the case of nitrogen-broadened
carbon dioxide by Yamamoto et al., (1968). They computed the wave-
length dependent broadening coefficient with respect to nitrogen at

10cm^{-1} intervals. Their results, the measurements of Burch et al.,
(1962), and the measurements made in this research are shown in
Figure 19. The theory seems to predict the general features of
the wavelength dependence of the self broadening coefficient rather
well. The theory seems to agree with the data of this investigation
better than with that of Burch et al., (1962) in the regions from
588 to 625cm^{-1} and from 714 to 770cm^{-1}. However, in the central
region (645 to 690cm^{-1}) the agreement with the data of Burch et al.
appears to be better.

There is one feature of the theoretical calculations that
seems inconsistent with the experimental results. Itappears that
where ever sharp peaks in the experimental data occur (615, 614,
and 722cm^{-1}), the theory predicts a decrease in the self-broadening
coefficient. The effect occurs at the three locations mentioned
and possibly also at 595cm^{-1} although the experimental peak is not
so pronounced there as it is at the other wavenumbers. The fact
that the theoretical calculations do not predict these peaks would
seem to indicate some difficulty with the theory.

7.6.6 The effect of line shape

The broadening coefficient depends on pressure, an effect which
is not predicted by a theory involving Lorentz shaped lines of
equal half width and a sharp peaking of the self-broadening coef-
ficient occurrs in the region of band centers which is not pre-
dicted by the line broadening theory of Anderson. The pressure
dependence, the sharp peaking near band centers and the rather
unusual behavior of helium might be explained if the shape of the

absorption lines depended upon the broadening gas. A heuristic arguement in favor of such an explanation is as follows. In the regions near the band centers, the centers of the individual absorption lines are very nearly opaque at the test conditions used here. In the regions away from the band centers this is not the case. Hence, as the broadening gas is added, much of the effect of the broadening gas in the vicinity of the band centers results from the change in absorption of the wings of lines that are located outside the region of the band center. In the regions between band centers the increasing absorption is a result of the increased absorption near the centers of the weaker non opaque lines located there. (It should be noted that many of the same effects could be produced by properly varying half widths.)

If this argument were valid, the ratio of the maximum broadening coefficient in the region of band centers to the minimum broadening coefficient between bands should be large for broadening gases producing lines with weak wings and small for broadening gases producing lines with strong wings. If this is the case, then, from the results obtained in this work data helium should broaden the wings of lines considerably less than would argon, nitrogen, or oxygen.

Although experimental measurements of the shape of carbon dioxide lines in the far wings ($\nu - \nu_0 > 10\alpha$) are relatively few, two different groups have obtained some data. Both of the investigations Burch et al., (1968) and Winters et al., (1964) used a similar method, which will be described below and their results will be discussed.

Essentially what is done is to locate a region in an absorption band where the absorption is caused by the wings of lines whose centers are outside the region, i.e., there are no lines centered in this region. If the positions and strengths of the lines in the band are known, an absorption spectrum for the band can be readily calculated. By comparing measured absorption spectra with absorption spectra which have been calculated for various line shapes the shape of the wings of the spectral lines can be empirically determined. In practice the high frequency wings of bands having sharp band heads have been used in these investigations.

Winters et al., (1964) have used this method to investigate the shapes of wings in the region from 2400 to 2600 cm^{-1}, for self-broadening and broadening by nitrogen and oxygen. Their results indicate that the wings are definitely sub-Lorentzian in this region for both self- and foreign gas broadening. The wings of the foreign gas broadened lines were weaker than the wings of the self-broadened lines. Nitrogen and oxygen produced results similar to each other. Experimental conditions were similar to those of this work.

Burch et al., (1968) used the same method to investigate the high frequency wings of the bands in the vicinity of 1.43 μm (7000cm^{-1}), 2.63 μm (3800cm^{-1}) and 4.3 μm(2350cm^{-1}). The shapes of the wings were investigated for self-broadening and for foreign gas broadening using argon, helium, hydrogen, nitrogen, and oxygen as broadening gases. Their results which were consistent in all of the bands, can be summarized as follows:

1. The wings of the self-broadened lines were definitely
    sub-Lorentzian, although not as much as had been found
    by Winters et al.

2. All foreign gases produced lines with weaker wings than
    wings than self-broadened lines.

3. The line shapes for nitrogen, argon, and oxygen were
    generally similar.

4. The line shapes for hydrogen and helium were similar,
    but the wings were considerably weaker than the wings
    of the nitrogen, argon, or oxygen broadened lines.

All of the above conclusions apply to the wings of the lines at
distances approximately 10 half widths or more from the line
center. They also found that the deviation from the Lorentzian
shape increased with decreasing wavenumber as one moved from band
to band.

If the same effects are assumed to hold for the 15 μm band of
carbon dioxide and, in addition, effects in the low frequency
wings of lines are assumed to be the same as those in the high
frequency wings, then the peaking of the broadening coefficient in
the band centers and the unusual behavior of helium relative to
that of argon, nitrogen, and oxygen might be a result of this dif-
ference in line shape.

7.6.7 Summary

In this section the wavelength dependent broadening coefficients
for carbon dioxide with respect to argon, helium, and nitrogen and
oxygen have been discussed. It has been concluded that the result

discussed in Chapter 6, viz, that helium and argon have similar band averaged broadening factors and that the broadening factor for oxygen is somewhat higher is verified by these data. It has been shown that the fine structure of the broadening coefficient versus wavelength curve is correlated with the presence of several absorption bands in the 15 μm (667cm^{-1}) region. The results for nitrogen broadening have been shown to be in fairly good agreement with other experimental measurements. The results for nitrogen broadening have also been compared with theory and it has been concluded that the theories are not adequate to predict the observed data. Finally, it has been concluded that line half widths that vary with rotational quantum number and broadening gas and line shapes that vary with broadening gas could have produced the observed results.

CHAPTER 8

CONCLUSIONS

8.1 Conclusions

As noted in Chapter 1, the experiments carried out in this investigation had as their object several goals. It was planned that these goals would be reached in such a manner that each step would lead to confidence in the results of the steps that followed. These goals (in order of discussion) were:

1. To obtain spectra in the 15 μm region for nitrogen broadened carbon dioxide samples for comparison with previous experimental work and with the theoretical calculations in the 15 μm band by Drayson and Young (1966) and Drayson et al., (1968).

2. To determine the band-averaged broadening coefficient for carbon dioxide with respect to nitrogen in the 15 μm region for comparison with other experimental determinations of this quantity.

3. To determine the band-averaged broadening factors with respect to nitrogen in the 15 μm region for argon, helium, and oxygen.

4. To investigate the wavelength dependence of the broadening coefficients for argon, helium, nitrogen, and oxygen in the 15 μm region.

The first two of the above items were performed primarily to determine whether or not the instrumentation system and data processing methods used would produce results that were in agreement with the work of others. Comparing the spectra obtained in this study

113

with those of Burch et al.,(1962) lead to the conclusion that the instrumentation system and data processing methods were satisfactory. The spectra were also compared with the calculations of Drayson and Young (1966) and Drayson et al.,(1968). It was evident that the calculations tended to overpredict the equivalent width for long path lengths, high equivalent pressures (near one atmosphere) and low concentrations of carbon dioxide. Although the comparisons were not complete enough to isolate the difficulties, they might be due to poor estimates of some band strengths and the use of a line shape (Lorentz) that overpredicts the absorption in the wings of foreign gas broadened lines.

Investigation of the band-averaged broadening factors showed that all the gases investigated (argon, helium, and oxygen) were less effective than nitrogen in broadening carbon dioxide absorption lines in the 15 μm region. These factors were not constant, but rather were weakly dependent on the gas pressure and the optical mass. Rather unexpectedly it was found that argon and helium were approximately equally effective on the average, for broadening the absorption lines. This result was different from that obtained by Burch et al.,(1962a) in their investigation of the 4.3 μm band where they found that helium was considerably less effective than argon. It did agree, however, with recently published data of Patty et al.,(1968) who found argon and helium to be of approximately equal effectiveness in the 10.6 μm region. Although the data of Patty, et al.,(1968) were obtained using a method that is quite different from the technique used in this study and that of Burch et al. they do substantiate the idea gained by comparing

the present work at 15μ m with the work of Burch et al., (1962a) at

$4.3\,\mu$m, that the effects of a broadening gas might be very different

in different absorption bands of an active gas. (This has been

noted previously by others, e.g., Coggeshall and Saier (1947) under

somewhat different conditons).

A check on the equality of the band-averaged coefficients for

argon and helium was carried out during the investigation of the

wavelength dependence of the broadening coefficients. This check

indicated that the band-averaged data were correct and that argon

and helium would be of approximately equal effectiveness, on the

average, for broadening carbon dioxide lines in the $15\,\mu$m region

in spite of the fact that the wavelength dependence of their broad-

ening coefficients was quite different.

It was found that the broadening coefficients for the different

gases were quite variable depending upon the wavelength. These

variations were least for argon ($\pm$ 10 percent of the mean value) and

greatest for helium ($\pm$ 30 percent of the mean value). The broad-

ening coefficients for the various gases tended to increase rather

sharply at particular wavelengths. It was shown that the positions

and heights of these peaks were correlated with the positions and

strengths of the stronger absoption bands in the region.

A dependence of the broadening coefficient on absorber partial

pressure or optical mass was discovered; this is contrary to the

work of Burch et al., (1962) in the $15\,\mu$m region for nitrogen. This

dependence was not investigated extensively and the effects of

optical mass and of pressure were not separated.

The wavelength dependent broadening coefficient for nitrogen was compared with the predictions of Anderson's theory (Anderson, 1949) as calculated by Yamamoto et al., (1968). The theory predicted the mean value and general shape of the wavelength dependent broadening coefficient rather well. It did, however, predict a decrease in the value of the broadening coefficient in each of the wavelength regions where a sharp peak in the value was found in the experimental data. On the basis of this comparison, it was concluded that the theory is not too satisfactory.

The possibility that the peaks were caused by a pressure broadened line shape that is sub-Lorentzian in the wings was discussed. Using a qualitative argument it was shown that such a line shape could produce the observed effect. It is known (Winters et al., (1964) and Burch et al., (1968) that the wings of foreign gas broadened lines in other carbon dioxide absorption bands are sub-Lorentzian. Unfortunately, however, much the same argument can be used to show that a band consisting of Lorentzian lines of properly varying half width might produce similar effects. We were not able to determine which, if either or both, of these mechanisms were present here. Further work will be required to determine the relative importance of these two effects.

8.2 Suggestions for future work

The results of this research have indicated that more theoretical and experimental work is needed in the 15 μm absorption band of carbon dioxide. Before the theory can be developed much further, however, it is likely that more experimental data must be obtained.

It now appears that the shape of the wings of the absorption
lines and the variation of the line half width with rotational
quantum number are the two most important areas which must be
investigated. Both of these appear to be variable depending upon
the composition of the broadening gas. The shapes of the far wings
of lines might be investigated by a method similar to that used by
Winters et al., (1964) and Burch et al., (1968). The measurement
will be more difficult (if at all possible) in the 15 um region
because of the presence of several overlapping bands in this region.
The variation of line half width with rotational quantum number
can probably be best investigated either by conventional high reso-
lution spectroscopy or possibly by some of the techniques that use
a tunable laser as a radiation source.

Using techniques similar to that used in this experimental
program one might determine the band-averaged and wavelength depen-
dent broadening factors for other broadening gases. Neon and
hydrogen would be of particular interest here. Since neon has a
polarizability between that of helium and argon one might be able
to determine whether or not the line width is proportional to some
collision frequency-polarizability product as has been suggested
by Patty, et al., (1968). Since hydrogen has been found to produce
a line shape in the far wings quite similar to that of helium, but
has an average broadening factor that is quite different in other
absorption bands of carbon dioxide, it would be of value to compare
the band average broadening factors and the wavelength dependent
broadening coefficients for these two gases in the 15 um region.

If the structure of the wavelength dependent broadening coefficient is caused by the presence of low absorption in the line wings we might expect the wavelength dependent broadening coefficients to be of generally similar form, but possibly of quite different mean value.

Theoretical calculations similar to those of Drayson and Young (1966) and Drayson et al., (1968) might be used to determine whether or not line shapes having sub-Lorentzian wings would produce the experimentally observed effects. This might be done by a point by point division of two spectra (one for pure carbon dioxide using Lorentz lines and the other for a carbon dioxide broadening gas mixture using a line shape having sub-Lorentzian wings.) This is, in essence, a simulation of the spectrophotometer as it operated during the determination of the wavenumber dependent broadening coefficient. On the basis of such calculations it might be possible to empirically determine the line shapes produced by the various broadening gases. These shapes could then be used to improve the accuracy of the techniques used for the inversion from atmosphere radiance profiles to atmospheric temperature profile.

BIBLIOGRAPHY

Anderson, A., A. Chai and D. Williams, 1967: Self broadening effects in the infrared bands of gases. J. Opt. Soc. Am., 57, 240-246.

Anderson, P. W., 1949: Pressure broadening in the microwave and infrared regions. Physical Review, 76, No. 5.

o
Angstrom, K., 1893: The quantitative determination of radiant heat by the method of electrical compensation. Phys. Rev. 1, 365.

o
Angstrom, K., 1901: Ueber die abhängigkeit der absorption der gase besonders de kohlensäure, von der dichte. Ann D. Physik, 6, 163.

o
Angstrom, K., 1908: Einige fundamentale sätze betreffs der absorption und der absorptionsspektren der gase. Arkiv. f. mathematik, Astronomi Och Fysik, 4, No. 30.

Benedict, W. S., R. Herman, G. E. Moore and S. Silverman, 1956a: The strengths, widths and shapes of infrared lines, Canadian Journal of Physics, 34, 830.

Benedict, W. S., R. Herman, G. E. Moore and S. Silverman, 1956b: The strengths, widths and shapes of infrared lines. Canadian Journal of Physics, 34, 850.

Benedict, W. S., R. Herman, G. E. Moore and S. Silverman, 1962: The strengths, widths and shapes of lines in the vibration-rotation bands of CO_2. Astrophysical Journal, 135, 277.

Boutin, R., D. Brulebois, C. Rosetti, 1967: Etude de la transition $00^{o}1-10^{o}0$ de N_2O. Influence d'un gaz perturbateur sur les largeurs des raies de vibration - rotation de la transition $00^{o}1-10^{o}0$ de CO_2. C. R. Acad. Sci. Paris, t. 265, 195-197.

Breene, R. C. 1961: The shift and shape of spectral lines. Pergamon Press, London, England.

Burch, D. E., D. Gryvnak, E. B. Singleton, W. L. France and D. Williams, 1962: Infrared absorption by CO_2, water vapor and minor atmospheric constituents. AFCRL-62-698, Air Force Cambridge Res. Labs.

Burch, D. E., E. B. Singleton, W. L. France and D. Williams, 1962a: Absorption line broadening in the infrared. Applied Optics, 1, 3.

Burch, D. E., D. Gryvnak, R. R. Patty, and C. E. Bartky, 1968: The shape of collision broadened CO_2 lines. Aeronutronic Division Philco-Ford Corp., Publication U-3203.

Chapman, S., Cowling, 1939: The Mathematical theory of non uniform gases. University Press, Cambridge, Mass.

Coggeshall, N. D. and E. L. Saier, 1947: Pressure broadening in the infrared and optical collision diameters. J. Chem. Phys., 15.

Crane-Robinson, C. and H. W. Thompson, 1963: Pressure broadening studies on vibration rotation bands III experimental methods for determining line widths. Proceedings of the Royal Society A 272, 441.

Drayson, S. R. and C. Young, 1965: Band strength and line half width of the 10.4μ CO_2 band. J. Q. S. R. T., 7, 993-995.

Drayson, S. R. and C. Young, 1966: Theoretical investigations of carbon dioxide radiative transfer. Univ. of Michigan, Report 07349-1-F.

Drayson, S. R., S. Y. Li and C. Young, 1968: Atmospheric absorption of carbon dioxide, water vapor and oxygen. Univ. of Michigan Report 08183-2-F. J.

Eaton, D. R. and H. W. Thompson, 1959: Pressure broadening studies on vibration rotation bands, I. the determination of line widths. Proc. Roy. Soc., 251.

Edwards, D. K., 1960: Absorption by infrared bands of carbon dioxide gas at elevated pressures and temperatures. J. Opt. Soc. Am., 50, 6.

Faddeeva, V. N. and N. M. Terentev, 1961: Tables of the probability integral for complex arguement. Pergamon Press, New York, N. Y.

Foley, H. M., 1946: The pressure broadening of spectral lines. Physical Review, 69, 616.

Fried, B. D. and S. D. Conte, 1961: The Plasma dispersion function. Academic Press.

Goody, L. M. and T. W. Wormell, 1951: The quantitative determination of atmospheric gases by infrared spectrosopic methods, I. laboratory determination of the absorption of the 7.8 and 8.6μ bands of nitrous oxide with dry air as a foreign gas. Proc. Roy. Soc., 209A, 178.

Goody, L. M., 1964: Atmospheric radiation - Theoretical basis. Oxford at the Clarendon Press.

Gordy, W., W. V. Smith and R. F. Trambarula, 1953: Microwave Spectroscopy. John Wiley and Sons, New York, N. Y.

Howard, J. N., D. E. Burch and D. Williams, 1956: Infrared transmission in synthetic atmospheres, II absorption by carbon dioxide. J. Opt. Soc. Am., 46, 4.

Howard R,, 1968: Private Communication.

Kuhn H., 1934: Pressure shift and broadening of spectral lines. Phil. Magazine, 18, 987.

Kuhn, H. and F. London, 1934: Limitation of the potential theory on the broadening of spectral lines Phil. Magazine, 18, 983.

Lindholm, E., 1945: Pressure broadening of spectral lines. Ark. Mat. Astron, Fysik, 32, 17.

Loeb, L. B., 1961: The kinetic Theory of Gases. Dover Publications, New York, N. Y.

Margenau, H. 1949: Pressure broadening in the inversion spectrum of amonia. Phys. Rev., 76, 121, 585A.

McCubbin, T. K. Jr. and T. R. Mooney, 1968: A study of the strengths and widths of lines in the 914 and 10.4μ m CO_2 bands. J. Q. S. R. T. ; 8, 1255-1264.

Michelson, A., 1895: On the broadening of spectral lines. Astrophys. J., 2, 4.

Nielson, J. R., V. Thornton and E. B. Dale, 1944: The absorption laws for gases in the infrared. Reviews of Modern Physics, 16, 34.

Patty, R. R., E. R. Manring and J. A Gardner, 1968: Determination of self broadening coefficients of CO_2, using CO_2 laser radiation at 10.6μ. Applied Optics, 7, 11.

Posener, D. W., 1959: The shape of spectral lines: Tables of the Voigt profile, Australian Journal of Physics, 12, 184.

Reule, A., 1968: Testing spectrophotometer linearity. Applied Optics, 7, 1023-1028.

Rossetti, C., F. Bourbonneux, R. Farrenq and P. Barchewitz, 1966: Optique Moleculaire avec source laser etude de la bands de CO_2 a 1064cm⁻1. Comtes Randus, 263 serie B, 241-243.

Townes, C. H. and A. L. Schawlow, 1955: Microwave spectroscopy. McGraw Hill Book Co., New York, N. Y.

Tsao, C. J. and B. Curnette, 1962: Line width of pressure broadened spectral lines. J. Q. S. R. T., 2, 41.

Van Vleck, J. H. and V. F. Weisskopf, 1945: On the shape of collision-broadened lines. Revs. Modern Phys., 17, 227.

Vasilevskii, K. P., V. A. Kabanov and T. E. Derviz, 1967: Intensity and half widths of CO_2 lines in the $4\nu_2 + \nu_3$ band. Optics and Spectroscopy, 23, 6.

Winters, B. 1963: Line shape in the wing beyond the band head of the 4.3μ band of CO_2. Scientific report number I, Physics Dept., Catholic Univ., Washington, D. C.

Winters, B., S. Silverman and W. Benedict, 1964: Line shape in the wing beyond the band head of the 4.3μ band of CO_2. J. Q. S. R. T., 4, 527-537.

Yamamoto, G., and T. Sasamori, 1958: Science Reports, Tohoku Univ., 5th Series (Geophysics) 10, 37.

Yamamoto, G., and T. Sasmori, 1964: Analysis of the 15μ CO_2 absorption measurements. Final Report under Contract Cwb-10548.

Yamamoto, G., M. Tanaka and T. Aoki, 1968: Estimation of the line widths of the 15μ CO_2 bands. Report of Tohoku Univ. Sendai, Japan.

Young, C., 1965a: Calculation of the absorption coefficient for lines with combined Doppler and Lorentz broadening. J. Q. S. R. T., 5, 549-552.

Young, C., 1965b: Tables for calculating the Voigt Profile. Univ. of Michigan Report 05863-7-T.